We thank the reviewers for carefully reading and critically thinking about this paper. Below are our responses to the reviewers' comments. Text from the main paper or supporting information are provided in italics with changes in the manuscript's text highlighted in yellow. Reviewer comments are bold and our responses are normal typeface.

Reviewer 1:
This paper presents measurements of particulate organic compounds made during the FIREX lab campaign with a novel multi-stage measurement technique. The compounds are identified or assigned to functional groups where possible. The dependence of the emission factors of OC, EC, and the different compound classes and individual compounds with modified combustion efficiency and fuel type are analyzed. This is an important piece of work that will further our efforts to understand the chemistry of organic aerosols from biomass burning smoke. The work appears to have been carefully done and important uncertainties and caveats are made clear. The conclusions are generally justified by the results presented. The paper, tables, and figures are also generally clear and well presented. I have no major concerns about the manuscript. Below I discuss a few minor issues that I would like the authors to address, and a few typos that need to be fixed.

P5, L31 and elsewhere: The numbers presented for the linear fits in this paragraph (including on page 6) do not match the numbers in Figure 1. Which set are correct? Please double-check all the numbers in the text to confirm they are consistent with the latest analysis of the data.

We have corrected these typos and have gone through the rest of the text to ensure the written slopes match those of the figures.

"EFs for OC and EC generally follow a logarithmic relationship such that log(EF$_{OC}$) is inversely proportional to MCE (slope of -9.506) and log(EF$_{EC}$) is directly proportional (slope 5.441). Comparison of the slopes suggests that decreasing MCE of a fire will produce an increasing amount of OC compared to EC. This is further confirmed by examining the ratio of OC to EC (OC/EC) with MCE. Figure 1(b) illustrates how OC/EC sharply increases with more smoldering fire conditions (slope of -16.555)."

P7, L9-18 and Figure 2: This may be outside the scope of this paper, but would it be possible to map the two axes of Figure 2 to the saturation vapor concentration, O/C ratio, or the hygroscopicity "kappa" parameter? If so, that would help modelers use this data more directly.
Though we completely agree that displaying the chromatogram in terms of C* or kappa would be helpful for modelers, this would fall outside the scope of this study. Converting GC retention times to C* has done before for underivatized compounds (i.e. non-polar compounds); we refer

the reviewer to Isaacman et al. (2011). However, this conversion method becomes more difficult and more uncertain for derivatized, polar compounds as each added trimethylsilyl group will alter the measured retention time and thus C*. A more accurate approach to estimate C* for these compounds can be found in Hatch et al. (2018).

Obtaining O/C ratio from our measurements would require assigning parent masses for all the observed compounds. Previous work from the Goldstein group has done this for underivatized organic compounds, i.e., mostly non-polar compounds with minimal functionality (Isaacman et al., 2011). However, compounds emitted from biomass burning tend to be highly functionalized with groups such as hydroxyl, amino, and thiols. To detect these compounds using GCxGC entails derivatization. Therefore, converting parent mass to a molecular formula would require knowledge of the number of derivatized functional groups and the identity of the polar functional groups. This is knowledge we do not have for the vast majority of compounds. A much more detailed examination of the fragmentation pattern observed in the VUV (i.e., soft ionization) mass spectra could be done to help determine the number of derivatization groups and potential functionality. However, this would be a time-intensive process and would still have extremely high uncertainty. As a result, we believe extracting O/C ratios from our observations would be would be far outside the scope of this paper but may be worthwhile in the future.

P8, L1-3: You mention the uncertainty in the organic nitrogen compounds, but what about the uncertainty in the other EFs? How should those be treated?
We have clarified that the uncertainty for classified, unidentified, non-organic nitrogen compounds is ~30% and expanded the discussion on why this value is lower than previously reported from our group (see (Zhang et al., 2018)). In contrast, we do not have much chemical information for the unknown compounds in general. As a result, we estimate the uncertainty to be a factor of 2. These uncertainties are stated in the SI where the calibration method is discussed more in depth.

Mass loading calibration curves were determined by measuring the instrument's response to varying amounts of 99 standard compounds typically found in biomass burning organic aerosol particles. We estimate the systematic uncertainty in the mass loadings for the unknown compounds at a factor of 2. Unidentified but classified compounds exhibited lower uncertainty due to similarities in instrument response to standards within the same family. To illustrate this reduction of uncertainty, we examine compounds with a RI of in the range of 1800-1900. Compounds that elute in this region include sugars, PAHs, aliphatics, and organic nitrogen. Their associated slopes from their mass loading calibration curves and compound family are provided in Table S2. Slopes within compound families are more similar than between families. For example, sugars exhibit slopes on average of 0.19 (not all shown in Table S2) whereas aliphatics have slopes of 1.1. An unclassified sample compound that elutes near myristic acid and galactose could be converted to mass loadings using either the slopes of myristic acid (0.43) or galactose (0.004). Depending which is chosen, the estimated mass

loading of this unclassified compounds could range over three orders of magnitude. However, if this sample compound were classified as a sugar, then the estimated mass loadings would be significantly higher and more in-line with the how typical sugars respond in the instrument. Our observations using various standard compounds indicate this calibration technique primarily lowers the uncertainty of more polar compounds to ±~30%.

Sampled compounds that exactly matched a standard compound have a lower uncertainty of ~±10% that is primarily due to instrument variation. Since the same data inversion factor was applied to the same observed compound across all samples, these systematic uncertainties do not affect the trends observed in this study but may affect the mass fractions each compound contributes to the total observed mass from a burn.

P8, L10-14: The "shrub" class has the most variation in EFs, and I'm wondering if that's because the plants also have the most biological diversity in that class? I could see where all pines are basically the same but shrubs can be very different from one another.

Yes, we agree with the reviewer that the shrubs likely exhibit the widest diversity in plant chemical composition compared to the other fuel classes. Differences between fuel chemical composition, as also seen with peat, leads to a wider range in observed EFs. We have added this to the main text.

Shrubs (MCE=0.92-0.98) exhibited the largest ranges in chemical family mass fractions (e.g., 0-42% organic nitrogen compounds and 2-43% substituted phenols), suggesting that plants in this fuel type are less similar to each other than coniferous fuels. This may be due to a wider range of plant chemical composition for shrubs than for the other fuel types. Overall, the I/SVOC mass fractions tend to be more similar for fuels within a fuel type with the most variation exhibited for fuel mixtures and shrubs.

P8, L17 and elsewhere: I agree that much of the variability in the EFs is due to MCE, but I think you understate the role of fuel type. It looks like the regression line is always low for conifers and always high for peat. I'd be curious what the effect of including fuel type as a factor variable in the linear regression would be (https://stats.idre.ucla.edu/r/modules/coding-for-categorical-variables-inregression-models/) and if it would improve the fit.

We agree with both reviewer 1 and 2 about the partial dependence of EFs on fuel type. However, we believe including fuel type as a co-variant would not be very useful for several reasons. (1) The number of plants within each fuel type except for the conifers and coniferous duff is low. This is simply due to the specific fuel samples chosen for burning during the Fire Lab studies.

We would require more burns of a broader range of plants within each fuel type in order more definitely establish fuel type as a co-variant. (2) Fuel type and MCE are not independent variables. Note from Figure 3, fuels within the same fuel type fall within a characteristic MCE window. This indicates that fuel type (and likely other factors such as moisture and geometry) and MCE are not independent variables, which would also complicate regression modeling. Though this suggestion from reviewer 1 and 2 is logical, we believe to accomplish this would be outside the scope of this study and could be a separate study in the future.

P9, L15: I don't understand the statement that "the predicted total I/SVOC EFs are on average higher than the measured EFs by a factor of 2." Isn't the point of a regression fit that "on average" the predicted value is the same as the measured value? How should I interpret this statement and the statements about the different fuel types?
We agree this is a confusing statement. We have changed it to clarify our point which is to highlight the differences between the model and particular fuel types. In addition, we have decided to present as a ratio of model to observed so the numbers have changed a bit.

The goodness-of-fit for the multi-fuel regression models can be evaluated by comparing the predicted EFs to those measured for the various fuel types in this study and others (Liu et al., 2017). As evident in Figure 4a, the predicted total I/SVOC to observed EFs are between 0.7-11 times higher for shrubs, 0.90-0.97 for grasses, 0.22-0.74 for conifers, 0.63-3.0 for coniferous duff, and 0.28-0.85 for woody debris.

P11, L17: I think this is the first time you discuss that the fuel structure of peat may be responsible for the difference, and I'm not sure you have any evidence for that statement, so I'd remove it from the conclusions.

We actually mention this is section 3.4 and cite Stockwell et al. (2016) since we are not the first to observe differences of peat with other fuels.

Figure 2 caption: "Size of a point approximately scales with its emission factor" – is this a quantitative mapping from a function of some sort? It's be nice if the supplemental data explained how the size of the point relate to EF, or if you added a point size scale to the legend.

Though the points do scale with EFs, we had to make corrections to the floor and ceiling limits of point sizes. This was done to prevent some points from dominating the entire area of the chromatogram and the minute points from fading from view. As a result, we cannot add a useful point scale size to the legend. However, we do mention in the main text that all the EFs as a function of MCE are provided in UCB-GLOBES. We have added this information to the supporting information (in section 3).

Table S6: That is a lot of significant figures given the error. Is there a reason you reported so many digits?

We have cut down the significant digits to better reflect the standard deviation.

	Shrubs	Grass	Wood	Coniferous Litter	Conifers	Peat	Dung	Coniferous Duff	Woody Debris
Unknown	50%, 5%	60%, 6%	50%, 14%	50%, 9%	60%, 13%	50%	50%	60%, 15%	88%, 1%
Non-cyclic aliphatics/oxy	10%, 9%	8%, 2%	8%, 2%	7%, 2%	6%, 2%	26%	9%	9%, 2%	1%, 0%
Sugars	10%, 3%	12%, 2%	20%, 8%	15%, 6%	20%, 10%	3%	14%	10%, 6%	5%, 1%
PAH/methyl+oxy	1%, 1%	0%, 0%	1%, 1%	2%, 0%	1%, 0%	1%	0%,	2%, 0%	1%, 0%
Resin acids /diterpenoids	0%, 0%	0%, 0%	0%, 0%	8%, 1%	3%, 2%	0%	0%	3%, 2%	0%, 0%
Sterols, triterpenoids	1%, 0%	0%, 0%	0%, 0%	1%, 0%	0%, 0%	0%	1%	0%, 0%	0%, 0%
Organic nitrogen	13%, 8%	12%, 1%	8%, 4%	14%, 1%	10%, 5%	15%	22%	11%, 6%	1%, 1%
Oxy aromatic heterocycles	1%, 2%	1%, 0%	1%, 0%	0%, 0%	1%, 0%	0%	0%	0%, 1%	0%, 0%
Oxy cyclics	0%, 0%	3%, 2%	0%, 0%	1%, 0%	1%, 1%	0%	1%	1%, 1%	0%, 0%
Methoxyphenols	3%, 1%	3%, 2%	7%, 3%	3%, 0%	2%, 1%	4%	3%	4%, 1%	3%, 1%
Substituted phenols	7%, 0%	1%, 0%	0%, 0%	1%, 0%	1%, 1%	1%	1%	1%, 0%	0%, 0%
Substituted benzoic acids	1%, 1%	0%, 0%	0%, 0%	0%, 0%	0%, 0%	0%	0%	0%, 0%	0%, 0%
Average MCE.	0.958	0.898	0.958	0.955	0.931	0.840	0.902	0.871	0.878

Typos:
P3, L10: Consider changing to "Therefore, a better representation"?

We have done this.

Therefore, a better or estimable representation of the chemical composition in smoke particles within models requires condensing the information from molecular-level speciation into useable relationships that correlate typical particle composition to a measurable burn variable.

P5, L7: "laser transmittance laser"?
We removed the second laser.

Section 3.2 heading and elsewhere: You don't need a colon at the end of headings
We have removed them.

Figure 4f: The other panels listed the R2 and equation below the chemical family name, but it is listed at the bottom here. Please make consistent..

We have tried to keep the labels consistent but were unable for some. This is due to space constraints where the label would overlap with a data point. Therefore, we had to switch the order of the label around to make it legible.

<u>Reviewer 2:</u>

Jen et al. have speciated particles and vapors from emissions of laboratory fires representative of those found in the Western US, as conducted at the Fire Sciences Lab in Missoula, MT. They performed 2D gas-chromatography/mass spectrometry to speciate a significant fraction of compounds from a whole range of organic families. Additionally, they were also able to develop log-linear regressions of the emission factors for these compounds with modified combustion efficiency (MCE) to aid development of fuel- and phase-specific emissions from fires in the Western US. The study is well motivated, the methods are appropriate, and the manuscript is well written. I had a few major comments surrounding the methods and data analysis. Regardless of my comments, I believe the speciation data from this study should help with modeling efforts to supplement the multi-agency ground, aircraft, and satellite based studies involving fires in the United States (e.g., WE-CAN, FIREX-AQ). I would like to recommend publication of this study in Atmospheric Chemistry and Physics after the authors have responded to the following major and minor comments.

Major comments:
1. Identification, Page 6, Section 3.2: Of the 3000 compounds measured across the 29 fires, 149 seem to be positively identified. These probably have the highest certainty amongst the speciated compounds. What fraction of the total speciated and total mass do these represent? I am sure they probably change with fuel type but it would still be nice to know the range and some basic statistics (mean, standard deviation).

This is an excellent suggestion. We have looked into this. The mass fractions of positively identified compounds range between 4-37% between the various burns (mean of 20% with a std of 9%). There does not appear to be a correlation of mass fractions of positively identified with

MCE. This is expected because which compounds are identified does not depend on combustion efficiency. We have added this quantification to the main text in section 3.2.

<mark>Identified compounds account for 4-37% of the total observed organic mass (mean of 20% with a standard deviation of 9%).</mark>

For the remaining (3000-149) compounds, the authors refer to the SI for a more complete description of the methodology used to identify these compounds. It seems like Section 5 in the SI is what the authors are referring to. I found this description to be unsatisfactory and I am not sure this is a useful guide for readers if there were to replicate your methodology for their own work.

We agree that there should be some form of algorithm developed to automatically classify compounds into chemical families. However, the signals in derivatized electron ionization mass spectra, retention times, and vacuum ultra-violet ionization mass spectra vary considerably between compounds within the same family. Close examination of all the available information and expert judgement allow identification of patterns within chemical families; some examples of the useful patterns are given in the section 5 of the. To our knowledge, no formal algorithm exists that is capable of combing through large chemical data set to organize compounds by families. There is clearly a need to develop such an algorithm but this falls outside the scope of this study.

What fraction of the total speciated and total mass do these remaining compounds account for, resolved by identified and unidentified?

The identified compounds (149 of them) account for 4-37% of the total observed mass. Classified compounds (~400 compounds), including identified compounds, account for 10-65% of the total observed mass (see Figure 3(a)). We did not measure the total mass which would also include inorganic species, black carbon, and non-volatile organic compounds (e.g., extremely low volatility organic compounds). These types of compounds would not thermally desorb off the filters and thus not be measured.

Finally, are the methods described herein common to analysis of GC/MS data and those of this research group? If they are, it would be beneficial to cite the group's earlier work in Section 3.2.
In general, our technique for identifying compounds is standard for GC/MS analysis in that we first compare the electron ionization mass spectra and first dimension retention index against the National Institute of Standards and Technology (NIST) mass spectral database. However, NIST MS Library contains only a small fraction of possible compounds and an even smaller fraction of possible derivatized compounds. As a result, our group developed a soft ionization technique to

help preserve the parent ion of these compounds for improved identification. This paper, Isaacman et al. (2012), has been cited in our main text. Furthermore, Worton et al. (2017a) have shown that even "great" matches with NIST mass spectral database (match factors above 900) still have a 14% chance of incorrect identification for underivatized compounds. Consequently, positive identification requires running a standard compound on the instrument to confirm identity. The method used to ID compounds here is a combination of comparing to NIST MS Library, parent ion mass, and standards and is shown in Table S1 in the ID Method column.

We have added the reference Worton et al. (2017) to the main text.

From those compounds, 149 compounds were identified using a combination of matching authentic standards (STD), RI, EI mass spectrum (via NIST mass spectral database, 2014 version), and VUV parent and fragment mass ions. True positive identification requires analyzing a standard compound on the instrument; however comparing the NIST match to parent mass determined from VUV mass spectrum analysis can also provide a level of identification (Worton et al., 2017b). Identified compounds account for 4-37% of the total observed organic mass (mean of 20% with a standard deviation of 9%). A table of these identified compounds with their identifying methods (e.g., standard matching, previous literature, or NIST mass spectral database), RI, 5 most abundant mass ions from the EI mass spectra, and fuel source(s) are given in Table S1.

2. Calibration, Page 5, lines 13-18: Has the calibration technique described here been validated to work? If yes, can you cite the most recent literature? If not, would it be possible to split the dataset to validate this technique? How well would it work? Also, what are typical uncertainties in using a projected calibration (e.g., nearest sugar standard or nearest eluting standard) to calculate masses?

The reviewer is correct in identifying the uncertainties involved with this calibration technique. The issue with calibrating unknown compounds is that assumptions must be made about their behavior in the instrument. Previous studies from our group have calibrated unknown compounds using the closest eluting (in both dimensions of the chromatogram) standard compound. We refer the reviewer to the SI of Zhang et al. (2018) and have added this reference to the text. Zhang et al. estimated the uncertainty to be ~40% though this value is likely higher for more polar compounds.

In an effort to reduce uncertainties, we have refined this approach to better include chemical information. We assume compounds of the same chemical family will behave similarly in the instrument. Thus, we decided to calibrate classified compounds with the nearest eluting standard compound from the same chemical family. To illustrate this reduction of uncertainty, we examine compounds with a first-dimension linear retention index of ~1800. Compounds that

elute in this region include sugars, PAHs, aliphatics, and organic nitrogen. Their associated slopes from their mass loading calibration curves and compound family are provided in the table below. Slopes within compound families are more similar than between families. For example, sugars exhibit slopes on average of 0.19 whereas aliphatics have slopes of 1.1. A sample compound that elutes near myristic acid and galactose may have estimated mass loadings over three orders of magnitude depending on which standard compound is used. However, if this sample compound were classified as a sugar, then the estimated mass loadings will be significantly lower and more in-line with the how typical sugars respond in the instrument. Our observations using various standard compounds indicate this calibration technique primarily lowers the uncertainty of more polar compounds (i.e., compounds that require derivatization) from previously unknown percentage to ~30%. Illustrative data for selected standards is in below table.

Compound Name	1st dimension retention index	2nd Dimension retention time (s)	Slopes from Mass Calibration	Compound Family
Octadecane (C18)	1831	0.260	1.70	Aliphatic
Mannose	1831	0.310	0.19	Sugar
Anthracene	1836	0.680	1.82	PAHs
Pinitol	1856	0.330	0.37	Sugar
5-Nitrovanillin	1866	1.350	0.67	Organic nitrogen
Myristic Acid (C14 acid)	1879	0.380	0.43	Aliphatic
Galactose	1885	0.320	0.004	Sugar

We have added this discussion into the supporting information, section 3.

Mass loading calibration curves were determined by measuring the instrument's response to varying amounts of 99 standard compounds typically found in biomass burning organic aerosol particles. We estimate the systematic uncertainty in the mass loadings for the unknown compounds at a factor of 2. Unidentified but classified compounds exhibited lower uncertainty due to similarities in instrument response to standards within the same family. To illustrate this reduction of uncertainty, we examine compounds with a RI of in the range of 1800-1900. Compounds that elute in this region include sugars, PAHs, aliphatics, and organic nitrogen. Their associated slopes from their mass loading calibration curves and compound family are provided in Table S2. Slopes within compound families are more similar than between families. For example, sugars exhibit slopes on average of 0.19 (not all shown in Table S2) whereas aliphatics have slopes of 1.1. An unclassified sample compound that elutes near myristic acid and galactose could be converted to mass loadings using either the slopes of myristic acid (0.43) or galactose (0.004). Depending which is chosen, the estimated mass

loading of this unclassified compounds could range over three orders of magnitude. However, if this sample compound were classified as a sugar, then the estimated mass loadings would be significantly higher and more in-line with the how typical sugars respond in the instrument. Our observations using various standard compounds indicate this calibration technique primarily lowers the uncertainty of more polar compounds to ±~30%.

Table S2 Example mass loading calibrations slopes for compounds in the RI=1800 range.

Compound Name	1D RI	2D retention time (s)	Mass Calibration Slopes	Compound Family
Octadecane (C18)	1831	0.260	1.70	Aliphatic
Mannose	1831	0.310	0.19	Sugar
Anthracene	1836	0.680	1.82	PAHs
Pinitol	1856	0.330	0.37	Sugar
5-Nitrovanillin	1866	1.350	0.67	Organic nitrogen
Myristic Acid (C14 acid)	1879	0.380	0.43	Aliphatic
Galactose	1885	0.320	0.004	Sugar

3. Fuel type as covariate, Sections 3.3-3.5: Despite the authors repeatedly saying that fuel type was an important covariate, they failed to account for it in the regression models and limited their modeling to one with just a single covariate (i.e., MCE). The regression models in Figures 4 and 5 clearly show that the model when blanket-ly applied to any fuel can over/underestimate the emissions for certain types of fuels. Please consider using fuel type as a covariate to see if the regression model can be improved.

The reviewer does point out an important observation of this study in that emission factors (EFs) of I/SVOCs does partially depend on fuel type. A notable example is coniferous fuels emitting high amounts of sugar compounds. Though the reviewer does suggest a valid way of improving the accuracy of our model by including dependence on fuel type, we have opted to not change our model for several reasons. First, relating EFs to MCE and fuel type is more complex than including fuel type as a covariant. Fuel type and MCE are not independent variables as fuel types can often burn within a characteristic range of MCE. For example, shrubs burned efficiently with MCE~0.97 and coniferous duff burned inefficiently with MCE~0.85. Furthermore, to include a robust analysis of EFs on fuel type would require significantly more emission samples within each fuel type that span a wider range of MCE. Though we conducted stack burns at the FIREX FSL campaign, we focused primarily on fuels found in the western US and only a handful of plants in each of the fuel types. We would need to burn similar fuels across a wider range of MCE and more fuels in general in order to better tease out the relationship of EFs with fuel type.

In real world modeling, the actual fuel type-specific measurements we present can be used if the fuels are known for a fire. However, the fuels, or mix thereof, are often unknown in which case our regression model provides a reasonable estimate for EFs of specific compounds or chemical families.

We have made this final point clearer in the conclusion of the main paper.

To provide modelers with useful relationships in estimating particle-phase I/SVOC emissions, logarithmic fits were applied to the measured EFs as a function of MCE. These regression models can be used to approximate EFs of I/SVOCs or their chemical families from average MCE of real wildfires <mark>*where fuel loadings, fuel types, and fuel mixtures are often unknown*</mark>.

4. OC for mass closure, Page 7, lines 9-10: How did the final observed mass on the filters compare to the OC measurements? Wouldn't the OC be the gold standard to test for mass closure? If it is, shouldn't Figure 3 be done by normalizing with OC? Further, can the mass distribution from OC1 through OC4 be another useful constraint on the identification and calibration techniques since the 1 through 4 OC types are crude approximations for decreasing vapor pressure species?

Organic carbon mass closure is the ultimate goal of speciated measurements of organic compounds in aerosol particles. We have carefully considered this during our data analysis however we stopped short of including an organic carbon to total observed I/SVOC comparison for two reasons: (1) converting organic carbon to organic aerosol is not trivial and (2) parent mass identification for all observed I/SVOCs is required. Organic carbon (OC) is often converted to organic mass (OM) using an empirically derived number between 1.4-1.7. Russell has shown that this number varies widely between samples collected from various locations (Russell, 2003). Aiken et al. provide ratios between 1.5-1.7 from Fire Lab burns of Lodgepole Pine and grass burns. The range of ratio values leads us to believe that we should determine our own OM/OC value as our TD-GCxGC VUV-EI/HRTOFMS can provide parent masses for all observed compounds. However, assigning parent masses using the VUV spectrum requires knowing the number of derivatized groups on the unknown organic compounds and which functional groups were derivatized (hydroxyl, amino, thiol). We currently have no method for determining these constraints. Furthermore, our technique sees a specific window of organic compounds (I/SVOCs) and does not include low volatility compounds which may account for a significant fraction of the organic carbon (~20% of total per May et al. (2013)). As stated in the main paper, collection onto quartz fiber filters likely includes gas-phase artifacts (i.e., VOCs) that would be seen by the OCEC analyzer but not by our GCxGC. We concluded from these reasons that we cannot easily compare OC to our total observed I/SVOC mass.

Comparing the OCEC thermograms to the retention time distributions of the GCxGC also cannot be done easily. This is due to the presence of VOCs on the filters which would impact the OCEC thermograms and the fact that we derivatize our compounds prior to GCxGC analysis. Derivatizing a compound will alter its volatility and therefore its retention time in the GCxGC.

With regards to OC being the gold standard: Studies have shown the measured OC and EC amounts (and thus the OC:EC ratio) is impacted by the measurement technique such as the transmittance and reflectance charring correction (see Chen et al. (2011) as an example). We hesitate to claim the OC measurement is a gold standard though it very likely has lower uncertainty values than our measured mass loadings from the GCxGC.

5. Gas/particle partitioning: Were C* identified/developed for these species? What phase are these species expected to be in inside a fire plume or near background concentrations of organic aerosol? The C* for the species could be provided in the SI.

Reviewer 1 mentions this same point. We completely agree that C* is a very useful parameter for the community. However, converting retention time/index into C* with derivatized compounds has not been done before and would likely lead to large errors in estimated C*. We refer the reviewer to Hatch et al. (2018) for a more accurate method in determining C*.

Minor comments:
1. Page 4, lines 10-11: If the quartz filters were the only ones analyzed in this study, I would state that after this sentence.
We have added this.

2. Page 4, line 18: Of the 75 fires, were only 29 sampled? Was there a reason the others were not?
Yes, 29 out of the 75 burns were analyzed. These 29 represent all the unique fuels burned, including several replicates and fuels from different collection locations to explore potential variability between burns of the same fuel. After examining the chromatograms of several replicate burns, we determined the variability between replicates was minor (except for fuels from a different location). Thus, we opted to not analyze the remaining 46 burns with the same level of detail as required for the presented analyses due to the large amount of time required. We have added this explanation to the text.

==Chromatograms from replicate burns showed minor variation thus the remaining 46 burns were not analyzed in detail.==

3. Page 5, line 11: Why is a data inversion needed and what is it? Mention briefly in the main text.

The GCxGC does not measure mass directly but rather provides a signal that is affected by matrix effects, instrument sensitivity, and other factors. Data inversion is needed to convert instrument signal to mass loadings (and subsequent emission factors). We have opted to change the text to remove confusion of using the word inversion.

Full details of the data ==conversion to mass loadings and emission factors with== its associated uncertainties are provided in the SI with important steps outlined here.

4. Page 7, lines 3-5: Does this library also contain the emission factors for all the species measured in this study? This would be a useful resource to share with the community. It would also be beneficial to list the emission factors for species by fire that contribute a significant amount of the total observed mass in the SI (e.g., levoglucosan).

Since numerous compounds are found in multiple burns, the library contains the EFs vs MCE relationships. We apologize for not including this in the library description and have now added it. These EF relationships have always been in UCB-GLOBES FIREX and now we have added it to the description.

This spectral library is compatible with NIST MS Search and contains mass spectra, n-alkane RI, potential compound identification or chemical families, ==EFs as a function of fire conditions,== and fuel sources of all unique compounds detected from the 29 analyzed burns.

Each separated compound's mass spectrum, n-alkane retention index, chemical family, ==EF vs. MCE relationship,== and fuel source are reported here in a publicly available mass spectral library (UCB-GLOBES FIREX) for future comparisons and identification of biomass burning organic compounds in atmospheric samples.

We have opted to not list the EFs for species that contribute a significant amount to the total observed mass in the SI because for most of the burns, these compounds are unknown and unclassified. However, we do believe this information is useful, so we have directed the reader in the "Data Sets" section to the open access data archives for NOAA FIREX where all of our observed EFs are given for each of the burns. This can be found at http://esrl.noaa.gov/csd/groups/csd7/measurements/2016firex/FireLab/DataDownload/.

UCB-GLOBES can be downloaded at the Goldstein website, https://nature.berkeley.edu/ahg/data/MSLibrary/. The specific library for FIREX is FSL_FIREX2016_vX.msp where X is the version number. The library contains information on all separated compounds observed during the FSL FIREX campaign in 2016 and will be periodically updated as compounds are matched across other campaigns. ==Observed emission factors for all of the observed compounds for each of the analyzed burns can be accessed for free==

5. Page 8, lines 13-14: Can this final point about similarity within fuels be made statistically?

This is a good suggestion though we believe this falls outside the scope of this study as we are more qualitatively comparing mass fractions between fuel types here. Our collaborators Lindsay Hatch and Kelley Barsanti at UC Riverside have two papers that more quantitatively compared compounds between fuel types: (Hatch et al., 2018) and a paper under review in EST.

6. Page 9, line 14: Is 'accuracy' the right word here? Since you are testing the fit to the data, you are looking at the 'goodness-of-fit'.
We agree and have changed this to goodness of fit.

The goodness-of-fit for the multi-fuel regression models can be evaluated by comparing the predicted EFs to those measured for the various fuel types in this study and others (Liu et al., 2017).

7. Figures 4 and 5: Consider adding a factor of 2, 5, or 10 envelope on here to bound the deviation of the data from the fit.

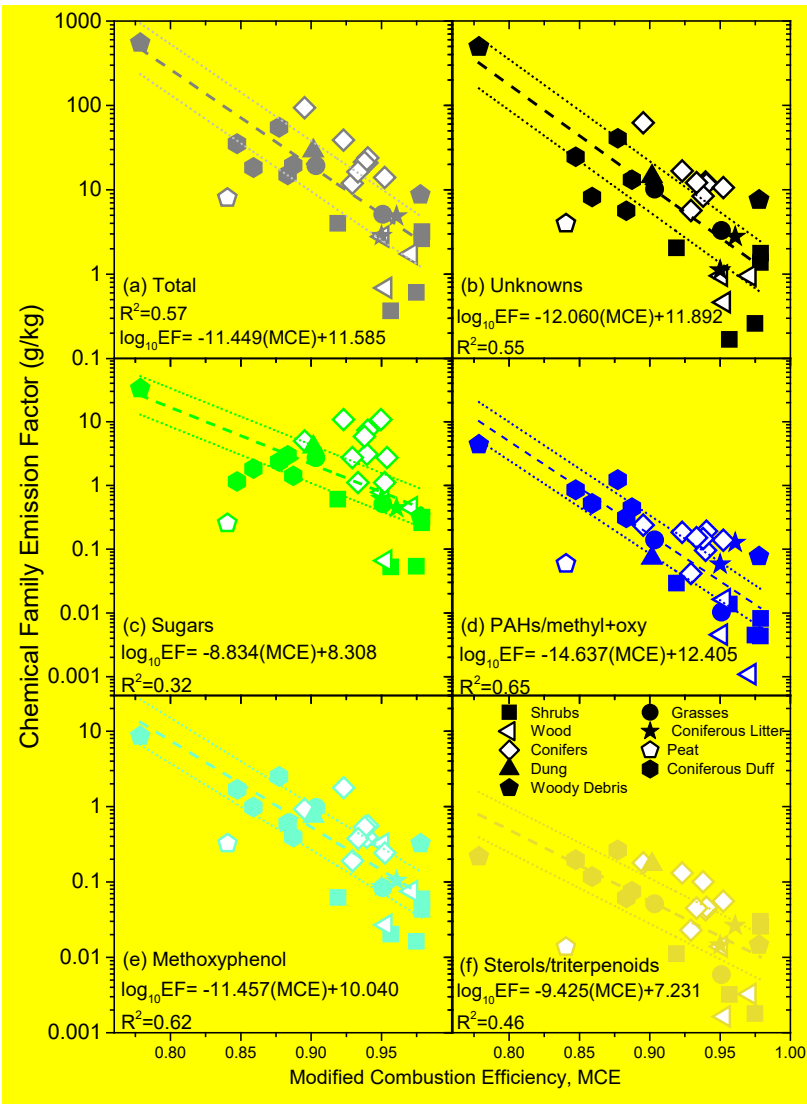We have added a plus/minus factor of 2 bounds to figure 4 and 5.

Figure 4 Summed emission factors (EFs) within a chemical family for each burn as a function of modified combustion efficiency (MCE). Each panel depicts a different family with (a) total observed I/SVOC EF, (b) unknowns, (c), sugars, (d) Polycyclic aromatic hydrocarbons (PAHs, including methylated and oxygenated forms), (e) methoxyphenols, and (f) sterols/triterpenoids. Dashed lines represent a log fit of the form log(EF) inversely proportional to MCE. The dotted lines represented a factor of 2 above and below the model. Symbols denote different fuel types.
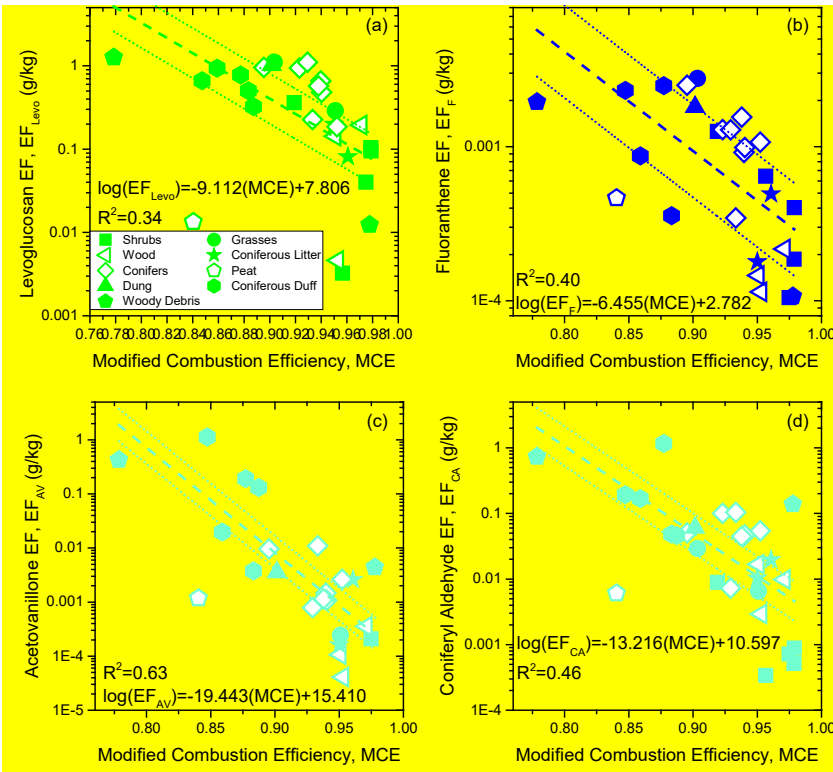
Figure 5 Emission factors (EFs) of (a) levoglucosan (sugar), (b) fluoranthene (PAH), (c) acetovanillone (methoxyphenol), (d) coniferyl aldehyde (methoxyphenol) for various fuel burns as a function of MCE. Dashed lines indicate a log fit of the form log(EF) inversely proportional to MCE. Dotted lines show a factor of 2 above and below the model. Note, peat (open pentagon) is not included in any of the fits. Different symbols represent fuel categories.

8. SI: The Selimovic et al. citation seems to have shown up as both the ACPD and ACP paper. Please correct.

We have fixed this.

9. SI, page 12: A sentence in this section says 'see SI for more details'. Self-referencing?

We have fixed this to refer to the next section.

References Cited:

Cheng, Y., He, K., Duan, F., Zheng, M., Du, Z., Ma, Y. and Tan, J.: Ambient organic carbon to elemental carbon ratios: Influences of the measurement methods and implications, Atmos. Environ., 45(12), 2060–2066, doi:10.1016/j.atmosenv.2011.01.064, 2011.

Hatch, L. E., Rivas-Ubach, A., Jen, C. N., Lipton, M., Goldstein, A. H. and Barsanti, K. C.: Measurements of I/SVOCs in biomass burning smoke using solid-phase extraction disks and two-dimensional gas chromatography, Atmos Chem Phys Discuss, Accepted, doi:https://doi.org/10.5194/acp-2018-863, 2018.

Isaacman, G., Worton, D. R., Kreisberg, N. M., Hennigan, C. J., Teng, A. P., Hering, S. V., Robinson, A. L., Donahue, N. M. and Goldstein, A. H.: Understanding evolution of product composition and volatility distribution through in-situ GC × GC analysis: a case study of longifolene ozonolysis, Atmos Chem Phys, 11(11), 5335–5346, doi:10.5194/acp-11-5335-2011, 2011.

Isaacman, G., Wilson, K. R., Chan, A. W. H., Worton, D. R., Kimmel, J. R., Nah, T., Hohaus, T., Gonin, M., Kroll, J. H., Worsnop, D. R. and Goldstein, A. H.: Improved resolution of hydrocarbon structures and constitutional isomers in complex mixtures using gas chromatography-vacuum ultraviolet-mass spectrometry, Anal. Chem., 84, 2335–2342, doi:10.1021/ac2030464, 2012.

Liu, X., Huey, L. G., Yokelson, R. J., Selimovic, V., Simpson, I. J., Müller, M., Jimenez, J. L., Campuzano-Jost, P., Beyersdorf, A. J., Blake, D. R., Butterfield, Z., Choi, Y., Crounse, J. D., Day, D. A., Diskin, G. S., Dubey, M. K., Fortner, E., Hanisco, T. F., Hu, W., King, L. E., Kleinman, L., Meinardi, S., Mikoviny, T., Onasch, T. B., Palm, B. B., Peischl, J., Pollack, I. B., Ryerson, T. B., Sachse, G. W., Sedlacek, A. J., Shilling, J. E., Springston, S., St. Clair, J. M., Tanner, D. J., Teng, A. P., Wennberg, P. O., Wisthaler, A. and Wolfe, G. M.: Airborne measurements of western U.S. wildfire emissions: Comparison with prescribed burning and air quality implications, J. Geophys. Res. Atmospheres, 122(11), 2016JD026315, doi:10.1002/2016JD026315, 2017.

May, A. A., Levin, E. J. T., Hennigan, C. J., Riipinen, I., Lee, T., Collett, J. L., Jimenez, J. L., Kreidenweis, S. M. and Robinson, A. L.: Gas-particle partitioning of primary organic aerosol emissions: 3. Biomass burning, J. Geophys. Res. Atmospheres, 118(19), 2013JD020286, doi:10.1002/jgrd.50828, 2013.

Russell, L. M.: Aerosol Organic-Mass-to-Organic-Carbon Ratio Measurements, Environ. Sci. Technol., 37(13), 2982–2987, doi:10.1021/es026123w, 2003.

Stockwell, C. E., Jayarathne, T., Cochrane, M. A., Ryan, K. C., Putra, E. I., Saharjo, B. H., Nurhayati, A. D., Albar, I., Blake, D. R., Simpson, I. J., Stone, E. A. and Yokelson, R. J.: Field measurements of trace gases and aerosols emitted by peat fires in Central Kalimantan, Indonesia, during the 2015 El Niño, Atmospheric Chem. Phys., 16(18), 11711–11732, doi:https://doi.org/10.5194/acp-16-11711-2016, 2016.

Worton, D. R., Decker, M., Isaacman-VanWertz, G., Chan, A. W. H., Wilson, K. R. and Goldstein, A. H.: Improved molecular level identification of organic compounds using comprehensive two-dimensional chromatography, dual ionization energies and high resolution mass spectrometry, Analyst, 142(13), 2395–2403, doi:10.1039/C7AN00625J, 2017a.

Worton, D. R., Decker, M., Isaacman-VanWertz, G., Chan, A. W. H., Wilson, K. R. and Goldstein, A. H.: Improved molecular level identification of organic compounds using comprehensive two-dimensional chromatography, dual ionization energies and high resolution mass spectrometry, Analyst, 142(13), 2395–2403, doi:10.1039/C7AN00625J, 2017b.

Zhang, H., Yee, L. D., Lee, B. H., Curtis, M. P., Worton, D. R., Isaacman-VanWertz, G., Offenberg, J. H., Lewandowski, M., Kleindienst, T. E., Beaver, M. R., Holder, A. L., Lonneman, W. A., Docherty, K. S., Jaoui, M., Pye, H. O. T., Hu, W., Day, D. A., Campuzano-Jost, P., Jimenez, J. L., Guo, H., Weber, R. J., Gouw, J. de, Koss, A. R., Edgerton, E. S., Brune, W., Mohr, C., Lopez-Hilfiker, F. D., Lutz, A., Kreisberg, N. M., Spielman, S. R., Hering, S. V., Wilson, K. R., Thornton, J. A. and Goldstein, A. H.: Monoterpenes are the largest source of summertime organic aerosol in the southeastern United States, Proc. Natl. Acad. Sci., 115(9), 2038–2043, doi:10.1073/pnas.1717513115, 2018.

Speciated and total emission factors of particulate organics from burning western U.S. wildland fuels and their dependence on combustion efficiency

Coty N. Jen[1,6*], Lindsay E. Hatch[2], Vanessa Selimovic[3], Robert J. Yokelson[3], Robert Weber[1], Arantza E. Fernandez[4], Nathan M. Kreisberg[4], Kelley C. Barsanti[2], Allen H. Goldstein[1,5]

[1] Department of Environmental Science, Policy, and Management, University of California, Berkeley, Berkeley, CA, 94720, USA

[2] Department of Chemical and Environmental Engineering and College of Engineering – Center for Environmental Research and Technology, University of California, Riverside, Riverside, CA, 92507, USA

[3] Department of Chemistry, University of Montana, Missoula, 59812, USA

[4] Aerosol Dynamics Inc., Berkeley, CA 94710, USA

[5] Department of Civil and Environmental Engineering, University of California, Berkeley, Berkeley, CA 94720, USA

[6] now at Department of Chemical Engineering, Carnegie Mellon University, Pittsburgh, PA 15213, USA

*correspond author: cotyj@andrew.cmu.edu

Abstract: Western U.S. wildlands experience frequent and large-scale wildfires which are predicted to increase in the future. As a result, wildfire smoke emissions are expected to play an increasing role in atmospheric chemistry while negatively impacting regional air quality and human health. Understanding the impacts of smoke on the environment is informed by identifying and quantifying the chemical compounds that are emitted during wildfires and by providing empirical relationships that describe how the amount and composition of the emissions change based upon different fire conditions and fuels. This study examined particulate organic compounds emitted from burning common western U.S. wildland fuels at the U.S. Forest Service Fire Science Laboratory. Thousands of intermediate and semi-volatile organic compounds (I/SVOCs) were separated and quantified into fire-integrated emission factors (EFs) using thermal desorption, two-dimensional gas chromatograph with online derivatization coupled to an electron ionization/vacuum ultra-violet high-resolution time of flight mass spectrometer (TD-GC×GC-EI/VUV-HRToFMS). Mass spectra, EFs as a function of modified combustion efficiency (MCE), fuel source, and other defining characteristics for the separated compounds are provided in the accompanying mass spectral library. Results show that EFs for total organic carbon (OC), chemical families of I/SVOCs, and most individual I/SVOCs span 2-5 orders of magnitude, with higher EFs at smoldering conditions (low MCE) than flaming. Logarithmic fits applied to the observations showed that log(EF) for particulate organic compounds were inversely proportional to MCE.

These measurements and relationships provide useful estimates of EFs for OC, elemental carbon (EC), organic chemical families, and individual I/SVOCs as a function of fire conditions.

1 Introduction

Wildfires in the western U.S. have become larger and more frequent, and this trend is expected to continue in the coming decades (Dennison et al., 2014; Miller et al., 2009). This is due to historical wildfire suppression leading to high fuel loading and climate changes that include longer springs and summers, earlier snow melts, and prolonged droughts (Dennison et al., 2014; Jolly et al., 2015; Spracklen et al., 2009; Westerling et al., 2006). Smoke emissions from wildfires primarily contain carbon dioxide (CO_2), carbon monoxide (CO), and thousands of organic compounds in the gas and particle phases. These organic compounds can significantly influence atmospheric chemistry, cloud formation, regional visibility, and human health. Thus, increased occurrences and magnitudes of wildfires will likely lead to greater smoke impacts on regional and global environments.

The extent to which smoke will adversely impact human health and the environment depends, in part, on the chemical composition and amount of emissions produced. In general, biomass burning, which includes wildfires, is the main global source of fine carbonaceous aerosol particles (~75%) in the atmosphere (Andreae and Merlet, 2001; Bond and Bergstrom, 2006; IPCC, 2014; Park et al., 2007). Individual and categorized organic emissions from wildfires have previously been identified and quantified (Akagi et al., 2011; Andreae and Merlet, 2001; Hatch et al., 2015; Kim et al., 2013; Koss et al., 2018; Liu et al., 2017; Mazzoleni et al., 2007; Naeher et al., 2007; Oros et al., 2006; Oros and Simoneit, 2001a; Simoneit, 2002; Stockwell et al., 2015; Yokelson et al., 2013). The bulk of previous studies on speciated organic compound emissions focused on gas-phase volatile organic compounds (VOCs). Particle-phase results are typically reported as total organic carbon (OC) or particulate matter (PM) with aerodynamic diameters less than 10 or 2.5 μm (PM_{10} and $PM_{2.5}$). These types of measurements provide no chemical specificity of the particle phase and thus limits the ability to predict how smoke will age in the atmosphere and impact the environment.

Several studies have examined specific particle-phase organic compounds in smoke such as toxic retene and other polycyclic aromatic hydrocarbons (PAHs) (e.g., Jayarathne et al., 2018; Kim et al., 2013; Naeher et al., 2007; Sullivan et al., 2014) or abundant tracer compounds, like levoglucosan and vanillic acid (Simoneit et al., 1999). Out of the likely thousands of unique compounds, roughly 400 known particle-phase organic compounds and their amounts produced per mass of dry fuel burned (a quantity known as the emission factor, EF) have been published and organized by wildland type (Oros et al., 2006; 2001a; 2001b). These compounds span many chemical families (i.e., functionalities), like sugars and methoxyphenols, and provide key insights into how different wildland burns lead to different organic particulate composition and EFs.

New advances in instrumentation, such as two-dimensional gas chromatography or electrospray ionization coupled to high resolution mass spectrometers (Isaacman et al., 2011; Laskin et al., 2009), now allow for unprecedented levels of molecular

speciation of atmospheric aerosol particles that can further identify and quantify the thousands of previously unreported biomass burning compounds. Nevertheless, current fire and atmospheric chemistry models that predict amount of smoke produced, its atmospheric transformation/transportation, and its physiochemical properties (e.g., French et al., 2011; Reinhardt et al., 1997; Wiedinmyer et al., 2011) do not model the thousands of organic compounds emitted from fires due

5   primarily to limited computational resources. To address this deficiency, Alvarado et al. (2015) used measured volatility distribution bins of organic compounds from fresh smoke and modeled their atmospheric aging by assuming shifts in volatility distribution via reactions with ozone and hydroxl radicals. Though this approach does better predict secondary organic aerosol particle formation, it still does not consider the wide variety of chemical compounds found in smoke, thus limiting its ability to predict physiochemical properties of aged smoke particles and their impacts on the environment.

10   Therefore, a better or estimable representation of the chemical composition in smoke particles within models requires condensing the information from molecular-level speciation into useable relationships that correlate typical particle composition to a measurable burn variable.

The purpose of this study is to (1) identify, classify, and quantify organic compounds in smoke particles produced during laboratory burns and (2) provide scalable EFs of individual compounds and their chemical families from various fuels as a

15   function of fire conditions. A selection of fuels and fuel combinations commonly consumed in western U.S. wildland fires was burned at the U.S. Forest Service Fire Sciences Laboratory (FSL) in Missoula, MT during the NOAA Fire Influence on Regional and Global Environments Experiment (FIREX) campaign in 2016 (Selimovic et al., 2018). Regression models representing EFs as a function of fire conditions are provided for groupings of organic compounds that vary in chemical complexity, from generalized organic carbon and total particulate organic compounds to specific chemical families and

20   individual compounds. In addition, a mass spectral database, compatible with the National Institute of Standards and Technology (NIST) Mass Spectral Search program, containing the mass spectra, retention indices, identities/compound classifications for all the separated compounds observed from the various burns is included. This database will be a valuable resource for the community for identifying specific chemicals in air masses impacted by biomass burning plumes and understanding the dominant source materials burned, fire characteristics, and atmospheric transformations.

25   **2 Materials and Methods**

Thirty-four different fuels were combusted in 75 "stack" burns during the 2016 FIREX campaign at FSL (Selimovic et al., 2018). Most fuels were representative of common biomass components found in the western U.S wildlands. Non-western U.S. wildland fuels were also burned and are used to demonstrate the applicability of the reported regression models across a wider range of fuels. A detailed description of the FSL combustion room can be found elsewhere (Christian et al., 2004;

30   Stockwell et al., 2014) with pertinent details described here. The 12.5 m × 12.5 m × 22 m combustion room contained a fuel bed on the floor. Fuels were placed in the fuel bed and ignited by resistance-heated coils. Above the fuel bed was a 3.6 m inverted funnel connected to a 1.6 m diameter exhaust stack that vented through the roof of the combustion room. The room

was kept at positive pressure to provide a constant air flow that diluted and carried the smoke up the stack. A platform was located 17 m above the fuel bed and allowed instrument sampling access into the stack (see Figure S1 in the supporting information, SI). The samples studied here were collected from the platform and thus represent fresh emissions.

Smoke from the stack was pulled through a custom-built sampler known as DEFCON, Direct Emission Fire CONcentrator (see diagram Figure S2 in SI). DEFCON's inlet was a 20.3 cm × 1.3 cm OD stainless steel tube that reached 15.2 cm into the stack. 10.3 LPM of smoke was pulled through the inlet, with two 150 ccm flows branching off from the main sample flow. These low-flow channels went to 2 parallel flows consisting of a Teflon filter followed by sorbent tube for gas-phase sample collection; analysis of those samples will be described in future publications. The remaining 10 LPM was passed through a 1.0 μm cutoff cyclone before being sampled onto a 10 cm quartz fiber filter (Pallflex Tissuquartz). Total residence time was ~2 s. One quartz fiber filter collected both particles and likely low volatility gases for the duration of each fire which lasted ~5-50 minutes. These filters were analyzed for this study. A few fires were terminated "early" when a small amount of fuel and smoldering combustion remained. Prior to collection, filters were baked at 550˚C for 12 hours and packed in similarly baked aluminum foil inside Mylar bags. The flows were monitored to ensure constant flow rates. Flow paths within DEFCON were passivated with Inertium® (Advanced Materials Components Express, Lemont, PA) which has been shown to reduce losses of oxygenated organics (Williams et al., 2006). After each burn, the inlet of DEFCON was replaced with a clean tube and the remainder of the system was purged with clean air. A background filter sample was collected each morning prior to the burns to estimate background contributions from sampling components and room air.

29 fire-integrated smoke filter samples, including one from each specific fuel (with some replicates), were selected and analyzed using a thermal desorption, two-dimensional gas chromatograph with online derivatization coupled to an electron ionization/vacuum ultra-violet ionization high-resolution time of flight mass spectrometer (TD-GC×GC-EI/VUV-HRToFMS) (Isaacman et al., 2012; Worton et al., 2017). A list of analyzed fuels are summarized in Table 1. Chromatograms from replicate burns showed minor variation thus the remaining 46 burns were not analyzed in detail. Punched samples of each filter (0.21-1.64 cm^2) were thermally desorbed at 320˚C under a helium flow using a thermal desorption system (TDS3 and TDSA2, Gerstel). Desorbed samples were then mixed with gaseous derivatization agent, MSFTA (N-methyl-N-trimethylsilyltrifluoroacetamide). MSFTA replaces the hydrogen in polar hydroxyl, amino, and thiol groups with trimethylsilyl group, creating a less polar and thus elutable compound. Derivatized samples then were focused on a quartz wool glass liner at 30˚C (cooled injection system, CIS4, Gerstel) before rapid heating to 320˚C for injection into the gas chromatograph (GC, Agilent 7890). GC×GC separation was achieved with a 60 m × 0.25 mm × 0.25 μm semi-nonpolar capillary column (Rxi-5Sil MS, Restek) followed by medium-polarity second dimension column (1 m × 0.25 mm × 0.25 μm, Rtx-200MS, Restek). A dual-stage thermal modulator (Zoex), consisting of a guard column (1 m × 0.25 mm, Rxi, Restek), was used to cryogenically focus the effluent from the first column prior to heated injection onto the second column (modulation period of 2.3 s). The main GC×GC oven ramped at 3.5°C/min from 40°C to 320°C and was held at the final temperature for 5 min and the secondary oven ramped at the same rate from 90°C to 330°C and held for 40 min. Separated

compounds were then ionized either by traditional EI (70 eV) or VUV light (10.5 eV). HRToFMS (ToFWerk) was used to detect the ions and was operated with a resolution of 4000 and transfer line and ionizer chamber temperatures at 270˚C. VUV light was provided by the Advanced Light Source, beamline 9.0.2, at Lawrence Berkeley National Laboratories. During the VUV experiments, the HRToFMS operated at a lower ionizer chamber temperature of 170˚C to further reduce molecular fragmentation (Isaacman et al., 2012).

Punches from the filter samples were also analyzed for organic and elemental carbon (OC and EC respectively) using a Sunset Model 5 Lab OCEC Aerosol Analyzer following the NIOSH870 protocol in the Air Quality Research Center at the University of California, Davis. Thermal pyrolysis (charring) was corrected using laser transmittance. OC and EC were also measured on the background filters.

2.1 Emission Factor Calculations

The mass loadings for all separated compounds measured by TD-GC×GC-EI/VUV-HRToFMS were determined using a set of calibration curves. Full details of the data conversion to mass loadings and emission factors with its associated uncertainties are provided in the SI with important steps outlined here. The TD-GC×GC-EI/VUV-HRToFMS responses to a wide range of standard compounds commonly found in biomass burning samples were measured at varying mass loadings to create calibration curves. Measured peaks from the filters were calibrated using a standard compound that exhibited similar first and second dimension retention times and compound classification. For example, a sampled compound classified as sugar was quantified using the nearest sugar standard compound in the chromatogram. Unknown compounds were matched to the nearest eluting standard compound, similar to the approach taken by Zhang et al. (2018). The mass loadings of all observed compounds were then background subtracted; however, the mass on the background filter for all compounds was negligible. The compound's emission factor ($EF_{compound}$) was then calculated by normalizing mass loadings by background-corrected sampled CO_2 mass. This ratio was then multiplied by the corresponding EF_{CO2}, as given in Selimovic et al. (2018). EFs for OC and EC were calculated similarly, using background-corrected OC and EC mass loadings.

3 Results and Discussion

3.1 Emission factors of organic and elemental carbon

OC and EC EFs were first related to the fire-integrated modified combustion efficiency (MCE). MCE reflects the mix of combustion processes in the fire and is defined as background-corrected values of $CO_2/(CO_2+CO)$ (Akagi et al., 2011; Ward and Radke, 1993). MCE values near 1 indicate almost pure flaming, while values near 0.8 are almost pure smoldering with 0.9 representing a roughly equal mix of these processes. Figure 1(a) shows the EFs of OC and EC (EF_{OC} and EF_{EC}) as a function of MCE across a variety of fuel types (see table 1). Decreasing MCE (more smoldering) results in increased OC and decreased EC emissions across all studied fuel types. These observed trends are in general agreement with previous studies (e.g., Christian et al., 2003; Hosseini et al., 2013). EFs for OC and EC generally follow a logarithmic relationship such that

log(EF_{OC}) is inversely proportional to MCE (slope of -9.506) and log(EF_{EC}) is directly proportional (slope 5.441). Comparison of the slopes suggests that decreasing MCE of a fire will produce an increasing amount of OC compared to EC. This is further confirmed by examining the ratio of OC to EC (OC/EC) with MCE. Figure 1(b) illustrates how OC/EC sharply increases with more smoldering fire conditions (slope of -16.555). This trend also follows a similar inversely proportional logarithmic relationship as EF_{OC} vs. MCE but with even stronger correlation (R^2=0.85 compared to 0.66, respectively). Note, values for Douglas Fir rotten log (burn 31), peat (burn 55), rice straw (burn 60), and Engelmann spruce duff (burn 26) fires are not shown due to measured EC at background levels. In addition, significant losses (~40%) of organic compounds were only observed for the Douglas Fir rotten log burn and was determined by comparing GC×GC chromatograms taken prior to OC/EC analysis (~2 years after collection) and ~1 month after collection at FSL. The combined results clearly show that flaming combustion produce slightly more particulate EC compared to OC whereas smoldering combustion emits 1-2 orders of magnitude higher levels of OC compared to EC.

3.2 Identification and quantification of I/SVOCs

Filter samples were analyzed for intermediate and semi-volatile organic compounds (I/SVOCs) using the TD-GC×GC EI-VUV-HRToFMS. Between 100-850 peaks (i.e., unique compounds) were separated in each fire-integrated chromatogram with fewer peaks observed for more flaming fires such as from shrub fuels (see Table 1). An example two-dimensional chromatogram of a lodgepole pine burn (burn 63) is shown in Figure 2. Based on the GC×GC configuration, all compounds elute between dodecane (C*~10^6 µg m^{-3} and an n-alkane retention index, RI, of 1200) and hexatriacontane (C*~10^{-1} µg m^{-3}, RI=3600) and thus are classified as I/SVOCs with a small fraction as low-volatility organic compounds (Donahue et al., 2009). In total, approximately 3000 unique compounds were separated across the 29 analyzed burns (see Table 1). From those compounds, 149 compounds were identified using a combination of matching authentic standards (STD), RI, EI mass spectrum (via NIST mass spectral database, 2014 version), and VUV parent and fragment mass ions. True positive identification requires analyzing a standard compound on the instrument; however comparing the NIST match to parent mass determined from VUV mass spectrum analysis can also provide a level of identification (Worton et al., 2017). Identified compounds account for 4-37% of the total observed organic mass (mean of 20% with a standard deviation of 9%). A table of these identified compounds with their identifying methods (e.g., standard matching, previous literature, or NIST mass spectral database), RI, 5 most abundant mass ions from the EI mass spectra, and fuel source(s) are given in Table S1.

To help reduce the chemical complexity from the 3000 observed compounds, each separated compound was sorted into a chemical family. This was achieved using a combination of parent ion mass (VUV), fragment ion mass spectra (VUV and EI), RI, and second-dimension retention time to estimate the compound's functionality. More details on the classification process and examples within each category can be found in the SI. The chemical families were broadly named and include non-cyclic aliphatic/oxygenated, sugars, PAHs/methylated+oxygenated, resin acids/diterpenoids, sterols/ triterpenoids, organic nitrogen, oxygenated aromatic heterocycles, oxygenated cyclic alkanes, methoxyphenols, substituted phenols, and

substituted benzoic acids. Almost 400 compounds, including the identified and most frequently observed compounds in the analyzed burns, were grouped into these families. The remainder of the compounds, which were both uncategorizable and unidentifiable, were placed into the unknown category. Figure 2 illustrates the chemical families (indicated by color) of all the separated compounds emitted from an example lodgepole pine burn.

5   Despite many compounds remaining unknown, their defining traits such as mass spectra or retention index (i.e., volatility) can be compared to atmospheric samples to help the community better define the composition of biomass-burning derived, particle-phase organic compounds. As such, all ~3000 observed compounds have been compiled into a publicly available mass spectral database and first reported here as the University of California, Berkeley- Goldstein Library of Organic Biogenic and Environmental Spectra (UCB-GLOBES) for FIREX (see SI). This spectral library is compatible with NIST

10   MS Search and contains mass spectra, *n*-alkane RI, potential compound identification or chemical families, ==EFs as a function of fire conditions,== and fuel sources of all unique compounds detected from the 29 analyzed burns.

3.3 Average observed I/SVOC composition

The masses of observed I/SVOCs from each chemical family were summed over each fire-integrated sample and normalized to either the total observed I/SVOC mass or total classified I/SVOC mass. Figure 3a illustrates mass fractions of the

15   unidentified and unclassified (unknown) compounds out of the total observed mass from the 29 analyzed burns. Mass fractions for each chemical family out of the total observed mass are given in Table S5. Unknowns represent ~35 to 90% of I/SVOCs mass emitted during the analyzed burns, with woody debris (rotten logs) exhibiting the highest mass fraction of unknowns (~90%). Since the compounds that make up the unknown mass fraction varied between burns, differences in the mass fractions between fuel types is not indicative of higher emissions of any particular compound. However, notably the

20   two woody debris burns showed similar unknown compounds (i.e., 99% of the unknown mass was of compounds found in both burns) but occurred under two different fire conditions (burn 13 at MCE=0.98 and burn 31 at MCE=0.78). In both cases, the unknown mass fractions were similar at 87-89%. This observation provides some indication that fuel type plays a larger role than MCE in determining the unknown organic mass fraction in smoke particles.

Given that the unknown compounds typically varied between burns, the mass of each classified chemical family was

25   normalized to the total observed classified mass (i.e., excluding the unknown mass) in order to better compare classified compounds between burns. These results are shown in Figure 3b. Conifers, coniferous litter, and wood exhibited the highest fraction of sugars (38%, 29%, and 44% respectively) compared to other fuels (between 6-30%). Furthermore, levoglucosan was the largest single contributor to the sugars for these burns and ranged from 10-40% of the total sugars. These observations are consistent with previous studies that have shown high levoglucosan emissions from cellulose-rich wood

30   samples (Mazzoleni et al., 2007; Simoneit et al., 1999). Coniferous fuels also emitted higher amounts of resin acids/diterpenoids (7%, 16%, 7%, and 3% for conifers, coniferous litter, coniferous duff, and woody debris respectively), as previously observed (Hays et al., 2002; Oros and Simoneit, 2001a; Schauer et al., 2001). Peat (from Indonesia) emitted the

largest fraction of aliphatic compounds (52%) compared to other fuels, in agreement with previous observations (George et al., 2016; Iinuma et al., 2007; Jayarathne et al., 2018). Manzanita burns produced the highest amounts of substituted phenols (34% of total classified mass compared to 1-4% for other fuels), mostly as hydroquinone (Hatch et al., In Prep. 2018; Jen et al., 2018). Organic nitrogen compounds, most of which were nitro-organics, also contributed significantly (up to 43%) to the total observed classified mass for all fuels. These compounds tend to absorb light (Laskin et al., 2015) and may contribute to observed brown carbon light absorption from these burns (Selimovic et al., 2018). However, it should be noted that the instrument is not as sensitive to this class of compounds. Thus, the EF uncertainty is high (factor of 2) for compounds that are not positively identified with a standard but are categorized as organic nitrogen.

Figure 3b also provides some evidence that fuels within the same type generally show similar mass fractions of chemical families. For example, conifers, which consist of a mixture of coniferous ecosystem fuel component (e.g., canopy, duff, litter, and twigs), exhibit relatively similar mass fractions with sugars accounting for 30-50%, 4-28% non-cyclic aliphatic, 13-30% organic nitrogen, 2-20% resin acid/diterpenoids, and 1-4% PAH/methyl+oxy across the MCE range of 0.90-0.95. Coniferous duff (MCE=0.85-0.89) exhibited lower sugar fraction (11-31%) but higher non-cyclic aliphatics 15-38% than the conifers. Burning grasses (MCE=0.90-0.95) produced roughly equal amounts of sugars and organic nitrogen compounds (30%) and higher amounts of oxygenated cyclic compounds (3-11%), like lactones, than the coniferous fuels. (~1%). Shrubs (MCE=0.92-0.98) exhibited the largest ranges in chemical family mass fractions (e.g., 0-42% organic nitrogen compounds and 2-43% substituted phenols), suggesting that plants in this fuel type are less similar to each other than coniferous fuels. This may be due to a wider range of plant chemical composition for shrubs than for the other fuel types. Overall, the I/SVOC mass fractions tend to be more similar for fuels within a fuel type with the most variation exhibited for fuel mixtures and shrubs.

3.4 EFs as a function of fire conditions (MCE)

Unlike the dependence of chemical family mass fractions on fuel type, EFs for each chemical family showed a correlation with MCE across all fuels examined and to a much lesser extent on fuel type. Figure 4 presents EFs for total observed organic compounds and 5 of the chemical families (unknowns, sugars, PAHs/methyl/oxy, methoxyphenols, and sterols/triterpenoids, with others given in Figure S4) as a function of MCE. Fuels not found in the western U.S. are also included in these figures to demonstrate that their EFs generally follow the trend with MCE. The notable exception is peat, a semi-fossilized fuel (Stockwell et al., 2016), whose EFs for all chemical families are roughly an order of magnitude lower than other fuels at similar MCE values, except non-cyclic aliphatic/oxygenated EF which is approximately equal to burns at similar MCE (see Figure S4). In general, EFs measured by the TD-GC×GC-EI/VUV-HRToFMS agree with previous literature (Hays et al., 2002; McDonald et al., 2000; Oros et al., 2006; Oros and Simoneit, 2001a, 2001b). For example, Oros and Simoneit (2001a) provided the sum of carboxylic acids and alkanes/enes/ols for conifer burns at ~1 g/kg, which is within our reported range 0.4-2.3 g/kg (MCE=0.90-0.95) for non-cyclic aliphatic/oxygenated emitted from burning conifers. Other

chemical family EFs presented here for conifers, including PAHs (0.4 g/kg), diterpenoids (1-3 g/kg), and methoxyphenols (1 g/kg), are also in good agreement with those published in Oros and Simoneit (2001a). Hays et al. (2002) reported EF for unknown compounds from ponderosa pine ~ 20 g/kg, higher than 11 g/kg (MCE=0.94) for the ponderosa pine burn studied here. This may be due to more compounds being classified here than in Hays et al. (2002) or differences in MCE between the studies. In contrast to previous work, EFs for chemical families reported here were measured over a wider range of fire conditions and fuel types and show a clear relationship with MCE.

Chemical family EFs span ~3 orders of magnitude and therefore logarithmic fits (given as a dashed line in the semi-log graphs of Figure 4) were applied to all the measurements excluding peat. Slopes range between -9.425 for sterols/triterpenoids to -14.637 for PAHs/methyl+oxy (fitted slopes, intercepts, and their errors for all chemical families are provided in Table S6). Three decimal places are provided for both the slope and intercept in order to reproduce the regression line. The R^2 values for the sugars (Figure 4) and resin acids/diterpenoids (Figure S4) are noticeably lower at 0.32 and 0.31, respectively, than the other chemical families (R^2~0.4). This is primarily due to the high mass fraction of sugars and resin acids/diterpenoids found in conifers, as stated above, and suggests that high emissions of both types of compounds are indicative of burning conifers. Also, coniferous litter emitted high amounts of resin acids/diterpenoids. Removing conifers from the semi-logarithmic model for sugars yields a $\log_{10}(EF_{sugars})$= -10.299(MCE)+9.361 with R^2=0.66 and removing conifers and coniferous litter for resin acids/diterpenoids results in $\log_{10}(EF_{resin})$= -19.598(MCE)+16.360 with R^2=0.77. These R^2 values are then more similar to those of other chemical families. In general, these results indicate that MCE can be used to estimate EFs for various chemical across of broad range of fuels, including those not found in the western U.S. wildlands except peat, with minimal dependence on fuel type.

The goodness-of-fit for the multi-fuel regression models can be evaluated by comparing the predicted EFs to those measured for the various fuel types in this study and others (Liu et al., 2017). As evident in Figure 4a, the predicted total I/SVOC to observed EFs are between 0.7-11 times higher for shrubs, 0.90-0.97 for grasses, 0.22-0.74 for conifers, 0.63-3.0 for coniferous duff, and 0.28-0.85 for woody debris. The model is also compared to previously reported EFs from wildfires. Specifically, Liu et al. (2017) reported MCE values from three different California wildfires and total organic aerosol (OA) particle EFs, which are the most equivalent to total I/SVOC EFs measured here (though at MCE values of <0.8, we observed higher IVOCs mass loadings in our chromatograms which would likely not be included in the OA EFs at lower particle mass loadings (May et al., 2013)). Liu et al. measured MCE values of 0.935, 0.877, and 0.923 with OA EFs of 23.3, 30.9, and 18.8 g/kg respectively. The model given in Figure 4a predicts total I/SVOC EFs of 8, 35, and 10 g/kg for those MCE values. The predicted EFs are within a factor of ~2-3, consistent with measured total I/SVOC EFs reported here. No other previous experiments report chemical family EFs from wildfires with corresponding MCE values thus the accuracy of applying the chemical family regressions cannot be evaluated at this time. Without this information, uncertainty in using the reported regression models in predicting EFs of various chemical families is estimated to be a factor of 3. However, this uncertainty in EFs is minor when compared to uncertainties in estimating the amount of fuel burned in large-scale carbon emission fire

models (French et al., 2011; Urbanski et al., 2011), which is primarily due to high spatial and temporal variations in fuel loadings and lack of observational data. Thus, these regressions can be used to approximate EFs of various chemical families for a wide range of fuels and fuel mixtures from measured MCE values.

Figure 5 shows the fire-integrated EFs of four specific compounds, levoglucosan (sugar), fluoranthene (PAH), acetovanillone (methoxyphenol), and coniferyl aldehyde (methoxyphenol), as a function of MCE. Acetovanillone and coniferyl aldehyde, both methoxyphenols, have been reported previously as tracers for lignin pyrolysis and levoglucosan (and more broadly sugars) from cellulose (Hawthorne et al., 1989; Oros and Simoneit, 2001a; Schauer et al., 2001; Simoneit, 2002). In addition, fluoranthene and other PAHs are known carcinogenic compounds (Boffetta et al., 1997; Kim et al., 2013). EFs for levoglucosan, the most widely reported particulate tracer compound for biomass burning (Mazzoleni et al., 2007; Simoneit et al., 1999; Sullivan et al., 2014), range between ~0.004-1 g/kg from this study. Hosseini et al. (2013) reported EF_{levo} for chaparral ecosystems at 0.02-0.1 g/kg, similar to EF_{levo} for shrubs measured (0.004-0.1) in this study. Schuaer et al. (2001) provided average EF_{levo} for pine trees at 1.4 g/kg, roughly a factor of 2 higher than the average 0.6 g/kg EF_{levo} for conifers of this study. Oros and Simoneit (2001a) examined levoglucosan emissions from various types of pine trees with an average EF_{levo} of 0.02 g/kg, a factor of 30 lower than reported here. Many reasons could explain this difference, such as different smoke sampling/filter extraction procedures and different MCE conditions during sampling. Regardless, the levoglucosan EFs reported in this study generally fall within the ranges measured by previous groups.

EFs for the compounds shown in Figure 5 span 2-5 orders of magnitude across fire conditions and fuels, including fuels found outside of the western U.S. Similar to the chemical family EFs, peat displays significantly lower EFs (factor of ~10) than the other fuels. Consequently, applied logarithmic fits, given as dashed lines in Figure 5, exclude peat. Slopes of these fits range from -6.455 to -19.443 for the four displayed compounds. Figure 5a also shows that the R^2 value for levoglucosan is the lowest (0.34) compared to the other compounds (0.40-0.63). This poorer correlation with MCE is similar to that seen for the sugar EFs in Figure 4c, where EFs from burning conifers were higher than the model predicted. Removing the conifers' levoglucosan EFs results in $\log(EF_{levo})$= -9.547 (MCE)+8.041 and improves the correlation (R^2=0.43). Nonetheless, these measurements suggest compound EFs do depend to some extent on fuel type in addition to MCE. However, the spread of measured EFs around the logarithmic fit in Figure 5 indicate a factor of 3 uncertainty in estimating EFs from MCE.

In addition to the well-known biomass burning particulate compounds shown in Figure 5, these measurements provide useful models to estimate EFs for hundreds of previously unreported compounds (not shown in Figure 5). These commonly detected compounds (i.e., found in >10 burns and occur in almost all fuel types) exhibited EFs that were inversely proportional to MCE. Regression parameters for compounds not displayed here are provided in the UCB-GLOBES FIREX mass spectral library. Many of these compounds still remain unidentified or unknown (see Figure 3) but are now quantified as a function of fire conditions. Future work can be done to identify these compounds and ultimately, with the use of these

regressions, estimate their contribution to I/SVOC mass in fresh smoke and model how they chemically transform in the atmosphere.

4 Conclusions

Smoke produced from burning a wide variety fuels, primarily from the western U.S. wildlands, was collected onto quartz fiber filters at the Fire Science Laboratory and analyzed for elemental and organic carbon. The organic carbon fraction was further separated, identified, classified, and quantified using TD-GC×GC-EI/VUV-HRToFMS with online derivatization. Each separated compound's mass spectrum, *n*-alkane retention index, chemical family, EF vs. MCE relationship, and fuel source are reported here in a publicly available mass spectral library (UCB-GLOBES FIREX) for future comparisons and identification of biomass burning organic compounds in atmospheric samples. Between 10-65% of the I/SVOC mass for each burn could be specifically identified or placed into a chemical family. Fuels within the same type tended to exhibit similar mass fractions, regardless of fire condition (as quantitated modified combustion efficiency, MCE). For example, similar unknown compounds accounted for ~90% of the total observed mass for the two woody debris burns (MCE=0.78-0.98). Conifers exhibited similar sugar and resin acid/diterpenoid mass fractions (out of total classified mass) of 30-50% and 2-20% respectively (MCE=0.90-0.95). Burns of coniferous duff (MCE=0.85-0.89) emitted higher classified mass fractions of methoxyphenols (6-18%) than conifers. Peat, a semi-fossilized fuel, displayed a high classified mass fraction of non-cyclic aliphatic/oxy compounds (52%). Shrubs showed the widest range in mass fractions, indicating fuels in this type were the most dissimilar.

Unlike mass fractions which depend primarily on fuel type, measured emission factors (EFs), classified into either organic carbon, chemical families, or specific compounds, primarily depended on fire conditions (MCE). Regardless of classification, EFs spanned 2-5 orders of magnitude from smoldering to flaming conditions. EFs were shown to follow an inversely proportional relationship to MCE across the wide variety of all fuels studied. However, peat EFs for chemical families (except non-cyclic aliphatic compounds) and specific compounds were approximately a factor of 10 lower than fuels at similar MCE values. This is likely due to significant differences in fuel structure of peat. Furthermore, conifers exhibited higher sugar (factor of 5) and levoglucosan (factor of 3) emissions compared to other fuels within the same MCE range. This indicates that fuel type and specific fuels plays some role in the EFs, though more minor compared to MCE. This is particularly true for nitrogen species and fuel-specific tracer compounds, i.e. compounds that are only emitted from a particular fuel, which will be discussed in a forthcoming paper. However, in general, EFs for these particulate compounds primarily depend on MCE and can be estimated from the fire conditions.

To provide modelers with useful relationships in estimating particle-phase I/SVOC emissions, logarithmic fits were applied to the measured EFs as a function of MCE. These regression models can be used to approximate EFs of I/SVOCs or their chemical families from average MCE of real wildfires where fuel loadings, fuel types, and fuel mixtures are often unknown. For example, comparison with Liu et al. (2017) shows the estimated particulate organics from the regression model to be

within a factor of 2-3 from those measured in that study. The comparison between predicted and previously measured EFs is affected by methodology, concentration regime, and the definitions of I/SVOC. Regardless, these regression models provide approximate EFs (within a factor of 3) of numerous chemical families and organic species as solely a function of fire conditions across a wide variety of fuels. These regressions will allow modelers and other experimentalist to better define the chemical composition of smoke particles emitted from wildland burns in the western U.S. and potentially other parts of the world.

5 Data Sets

UCB-GLOBES can be downloaded at the Goldstein website, https://nature.berkeley.edu/ahg/data/MSLibrary/. The specific library for FIREX is FSL_FIREX2016_vX.msp where X is the version number. The library contains information on all separated compounds observed during the FSL FIREX campaign in 2016 and will be periodically updated as compounds are matched across other campaigns. Observed emission factors for all of the observed compounds for each of the analyzed burns can be accessed for free through the NOAA FIREX data archives (http://esrl.noaa.gov/csd/groups/csd7/measurements/2016firex/FireLab/DataDownload/).

6 Author Contributions

CNJ, LEH, VS, RJY, NMK, KCB, and AHG formulated the science question and designed the experimental setup. CNJ, LEH, VS, RJY, and AEF collected the data at FSL. CNJ and AHG analyzed the I/SVOC data. VS and RJY analyzed the CO and CO_2 data. RW organized the ALS campaign. CNJ wrote the manuscript with all authors contributing comments.

7 Acknowledgements

8 Competing Interests:

Authors declare that they have no conflict of interest.

References

Akagi, S. K., Yokelson, R. J., Wiedinmyer, C., Alvarado, M. J., Reid, J. S., Karl, T., Crounse, J. D. and Wennberg, P. O.: Emission factors for open and domestic biomass burning for use in atmospheric models, Atmos Chem Phys, 11(9), 4039–4072, doi:10.5194/acp-11-4039-2011, 2011.

5   Alvarado, M. J., Lonsdale, C. R., Yokelson, R. J., Akagi, S. K., Coe, H., Craven, J. S., Fischer, E. V., McMeeking, G. R., Seinfeld, J. H., Soni, T., Taylor, J. W., Weise, D. R. and Wold, C. E.: Investigating the links between ozone and organic aerosol chemistry in a biomass burning plume from a prescribed fire in California chaparral, Atmospheric Chem. Phys., 15(12), 6667–6688, doi:https://doi.org/10.5194/acp-15-6667-2015, 2015.

Andreae, M. O. and Merlet, P.: Emission of trace gases and aerosols from biomass burning, Glob. Biogeochem. Cycles, 10   15(4), 955–966, doi:10.1029/2000GB001382, 2001.

Boffetta, P., Jourenkova, N. and Gustavsson, P.: Cancer risk from occupational and environmental exposure to polycyclic aromatic hydrocarbons, Cancer Causes Control, 8(3), 444–472, doi:10.1023/A:1018465507029, 1997.

Bond, T. C. and Bergstrom, R. W.: Light Absorption by Carbonaceous Particles: An Investigative Review, Aerosol Sci. Technol., 40(1), 27–67, doi:10.1080/02786820500421521, 2006.

15   Christian, T. J., Kleiss, B., Yokelson, R. J., Holzinger, R., Crutzen, P. J., Hao, W. M., Saharjo, B. H. and Ward, D. E.: Comprehensive laboratory measurements of biomass-burning emissions: 1. Emissions from Indonesian, African, and other fuels, J. Geophys. Res. Atmospheres, 108(D23), 0148–0227, doi:10.1029/2003JD003704, 2003.

Christian, T. J., Kleiss, B., Yokelson, R. J., Holzinger, R., Crutzen, P. J., Hao, W. M., Shirai, T. and Blake, D. R.: Comprehensive laboratory measurements of biomass-burning emissions: 2. First intercomparison of open-path FTIR, PTR-20   MS, and GC-MS/FID/ECD, J. Geophys. Res. Atmospheres, 109(D2), D02311, doi:10.1029/2003JD003874, 2004.

Dennison, P. E., Brewer, S. C., Arnold, J. D. and Moritz, M. A.: Large wildfire trends in the western United States, 1984–2011, Geophys. Res. Lett., 41(8), 2014GL059576, doi:10.1002/2014GL059576, 2014.

Donahue, N. M., Robinson, A. L. and Pandis, S. N.: Atmospheric organic particulate matter: From smoke to secondary organic aerosol, Atmos. Environ., 43(1), 94–106, doi:10.1016/j.atmosenv.2008.09.055, 2009.

25   French, N. H. F., de Groot, W. J., Jenkins, L. K., Rogers, B. M., Alvarado, E., Amiro, B., de Jong, B., Goetz, S., Hoy, E., Hyer, E., Keane, R., Law, B. E., McKenzie, D., McNulty, S. G., Ottmar, R., Pérez-Salicrup, D. R., Randerson, J., Robertson, K. M. and Turetsky, M.: Model comparisons for estimating carbon emissions from North American wildland fire, J. Geophys. Res. Biogeosciences, 116(G00K05), doi:10.1029/2010JG001469, 2011.

George, I. J., Black, R. R., Geron, C. D., Aurell, J., Hays, M. D., Preston, W. T. and Gullett, B. K.: Volatile and semivolatile 30   organic compounds in laboratory peat fire emissions, Atmos. Environ., 132, 163–170, doi:10.1016/j.atmosenv.2016.02.025, 2016.

Hatch, L. E., Luo, W., Pankow, J. F., Yokelson, R. J., Stockwell, C. E. and Barsanti, K. C.: Identification and quantification of gaseous organic compounds emitted from biomass burning using two-dimensional gas chromatography–time-of-flight mass spectrometry, Atmos Chem Phys, 15(4), 1865–1899, doi:10.5194/acp-15-1865-2015, 2015.

35   Hatch, L. E., Rivas-Ubach, A., Jen, C. N., Lipton, M., Goldstein, A. H. and Barsanti, K. C.: Measurements of I/SVOCs in biomass burning smoke using solid-phase extraction disks and two-dimensional gas chromatography, Atmos Chem Phys Discuss, Accepted, doi:https://doi.org/10.5194/acp-2018-863, 2018.

Hawthorne, S. B., Krieger, M. S., Miller, D. J. and Mathiason, M. B.: Collection and quantitation of methoxylated phenol tracers for atmospheric pollution from residential wood stoves, Environ. Sci. Technol., 23(4), 470–475, doi:10.1021/es00181a013, 1989.

Hays, M. D., Geron, C. D., Linna, K. J., Smith, N. D. and Schauer, J. J.: Speciation of Gas-Phase and Fine Particle Emissions from Burning of Foliar Fuels, Environ. Sci. Technol., 36(11), 2281–2295, doi:10.1021/es0111683, 2002.

Hosseini, S., Urbanski, S. P., Dixit, P., Qi, L., Burling, I. R., Yokelson, R. J., Johnson, T. J., Shrivastava, M., Jung, H. S., Weise, D. R., Miller, J. W. and Cocker, D. R.: Laboratory characterization of PM emissions from combustion of wildland biomass fuels, J. Geophys. Res. Atmospheres, 118(17), 9914–9929, doi:10.1002/jgrd.50481, 2013.

Iinuma, Y., Brüggemann, E., Gnauk, T., Müller, K., Andreae, M. O., Helas, G., Parmar, R. and Herrmann, H.: Source characterization of biomass burning particles: The combustion of selected European conifers, African hardwood, savanna grass, and German and Indonesian peat, J. Geophys. Res. Atmospheres, 112(D8), doi:10.1029/2006JD007120, 2007.

IPCC: Climate Change 2014: Impacts, Adaptation, and Vulnerability. Part A: Global and Sectoral Aspects. Contribution of Working Group II to the Fifth Assessment Report of the Intergovernmental Panel on Climate Change [Field, C.B., V.R. Barros, D.J. Dokken, K.J. Mach, M.D. Mastrandrea, T.E. Bilir, M. Chatterjee, K.L. Ebi, Y.O. Estrada, R.C. Genova, B. Girma, E.S. Kissel, A.N. Levy, S. MacCracken, P.R. Mastrandrea, and L.L. White (eds.)], Cambridge University Press, Cambridge, United Kingdom and New York, NY, USA., 2014.

Isaacman, G., Worton, D. R., Kreisberg, N. M., Hennigan, C. J., Teng, A. P., Hering, S. V., Robinson, A. L., Donahue, N. M. and Goldstein, A. H.: Understanding evolution of product composition and volatility distribution through in-situ GC × GC analysis: a case study of longifolene ozonolysis, Atmos Chem Phys, 11(11), 5335–5346, doi:10.5194/acp-11-5335-2011, 2011.

Isaacman, G., Wilson, K. R., Chan, A. W. H., Worton, D. R., Kimmel, J. R., Nah, T., Hohaus, T., Gonin, M., Kroll, J. H., Worsnop, D. R. and Goldstein, A. H.: Improved resolution of hydrocarbon structures and constitutional isomers in complex mixtures using gas chromatography-vacuum ultraviolet-mass spectrometry, Anal. Chem., 84, 2335–2342, doi:10.1021/ac2030464, 2012.

Jayarathne, T., Stockwell, C. E., Bhave, P. V., Praveen, P. S., Rathnayake, C. M., Islam, M. R., Panday, A. K., Adhikari, S., Maharjan, R., Goetz, J. D., DeCarlo, P. F., Saikawa, E., Yokelson, R. J. and Stone, E. A.: Nepal Ambient Monitoring and Source Testing Experiment (NAMaSTE): emissions of particulate matter from wood- and dung-fueled cooking fires, garbage and crop residue burning, brick kilns, and other sources, Atmos Chem Phys, 18(3), 2259–2286, doi:10.5194/acp-18-2259-2018, 2018.

Jen, C. N., Liang, Y., Hatch, L. E., Kreisberg, N. M., Stamatis, C., Kristensen, K., Battles, J. J., Stephens, S. L., York, R. A., Barsanti, K. C. and Goldstein, A. H.: High Hydroquinone Emissions from Burning Manzanita, Environ. Sci. Technol. Lett., doi:10.1021/acs.estlett.8b00222, 2018.

Jolly, W. M., Cochrane, M. A., Freeborn, P. H., Holden, Z. A., Brown, T. J., Williamson, G. J. and Bowman, D. M. J. S.: Climate-induced variations in global wildfire danger from 1979 to 2013, Nat. Commun., 6, 7537, doi:10.1038/ncomms8537, 2015.

Kim, K.-H., Jahan, S. A., Kabir, E. and Brown, R. J. C.: A review of airborne polycyclic aromatic hydrocarbons (PAHs) and their human health effects, Environ. Int., 60(Supplement C), 71–80, doi:10.1016/j.envint.2013.07.019, 2013.

Koss, A. R., Sekimoto, K., Gilman, J. B., Selimovic, V., Coggon, M. M., Zarzana, K. J., Yuan, B., Lerner, B. M., Brown, S. S., Jimenez, J. L., Krechmer, J., Roberts, J. M., Warneke, C., Yokelson, R. J. and Gouw, J. de: Non-methane organic gas

emissions from biomass burning: identification, quantification, and emission factors from PTR-ToF during the FIREX 2016 laboratory experiment, Atmospheric Chem. Phys., 18(5), 3299–3319, doi:https://doi.org/10.5194/acp-18-3299-2018, 2018.

Laskin, A., Smith, J. S. and Laskin, J.: Molecular Characterization of Nitrogen-Containing Organic Compounds in Biomass Burning Aerosols Using High-Resolution Mass Spectrometry, Environ. Sci. Technol., 43(10), 3764–3771, doi:10.1021/es803456n, 2009.

Laskin, A., Laskin, J. and Nizkorodov, S. A.: Chemistry of Atmospheric Brown Carbon, Chem. Rev., 115(10), 4335–4382, doi:10.1021/cr5006167, 2015.

Liu, X., Huey, L. G., Yokelson, R. J., Selimovic, V., Simpson, I. J., Müller, M., Jimenez, J. L., Campuzano-Jost, P., Beyersdorf, A. J., Blake, D. R., Butterfield, Z., Choi, Y., Crounse, J. D., Day, D. A., Diskin, G. S., Dubey, M. K., Fortner, E., Hanisco, T. F., Hu, W., King, L. E., Kleinman, L., Meinardi, S., Mikoviny, T., Onasch, T. B., Palm, B. B., Peischl, J., Pollack, I. B., Ryerson, T. B., Sachse, G. W., Sedlacek, A. J., Shilling, J. E., Springston, S., St. Clair, J. M., Tanner, D. J., Teng, A. P., Wennberg, P. O., Wisthaler, A. and Wolfe, G. M.: Airborne measurements of western U.S. wildfire emissions: Comparison with prescribed burning and air quality implications, J. Geophys. Res. Atmospheres, 122(11), 2016JD026315, doi:10.1002/2016JD026315, 2017.

May, A. A., Levin, E. J. T., Hennigan, C. J., Riipinen, I., Lee, T., Collett, J. L., Jimenez, J. L., Kreidenweis, S. M. and Robinson, A. L.: Gas-particle partitioning of primary organic aerosol emissions: 3. Biomass burning, J. Geophys. Res. Atmospheres, 118(19), 2013JD020286, doi:10.1002/jgrd.50828, 2013.

Mazzoleni, L. R., Zielinska, B. and Moosmüller, H.: Emissions of Levoglucosan, Methoxy Phenols, and Organic Acids from Prescribed Burns, Laboratory Combustion of Wildland Fuels, and Residential Wood Combustion, Environ. Sci. Technol., 41(7), 2115–2122, doi:10.1021/es061702c, 2007.

McDonald, J. D., Zielinska, B., Fujita, E. M., Sagebiel, J. C., Chow, J. C. and Watson, J. G.: Fine Particle and Gaseous Emission Rates from Residential Wood Combustion, Environ. Sci. Technol., 34(11), 2080–2091, doi:10.1021/es9909632, 2000.

Miller, J. D., Safford, H. D., Crimmins, M. and Thode, A. E.: Quantitative Evidence for Increasing Forest Fire Severity in the Sierra Nevada and Southern Cascade Mountains, California and Nevada, USA, Ecosystems, 12(1), 16–32, doi:10.1007/s10021-008-9201-9, 2009.

Naeher, L. P., Brauer, M., Lipsett, M., Zelikoff, J. T., Simpson, C. D., Koenig, J. Q. and Smith, K. R.: Woodsmoke Health Effects: A Review, Inhal. Toxicol., 19(1), 67–106, doi:10.1080/08958370600985875, 2007.

Oros, D. R. and Simoneit, B. R. T.: Identification and emission factors of molecular tracers in organic aerosols from biomass burning Part 1. Temperate climate conifers, Appl. Geochem., 16(13), 1513–1544, doi:10.1016/S0883-2927(01)00021-X, 2001a.

Oros, D. R. and Simoneit, B. R. T.: Identification and emission factors of molecular tracers in organic aerosols from biomass burning Part 2. Deciduous trees, Appl. Geochem., 16(13), 1545–1565, doi:10.1016/S0883-2927(01)00022-1, 2001b.

Oros, D. R., Abas, M. R. bin, Omar, N. Y. M. J., Rahman, N. A. and Simoneit, B. R. T.: Identification and emission factors of molecular tracers in organic aerosols from biomass burning: Part 3. Grasses, Appl. Geochem., 21(6), 919–940, doi:10.1016/j.apgeochem.2006.01.008, 2006.

Park, R. J., Jacob, D. J. and Logan, J. A.: Fire and biofuel contributions to annual mean aerosol mass concentrations in the United States, Atmos. Environ., 41(35), 7389–7400, doi:10.1016/j.atmosenv.2007.05.061, 2007.

Reinhardt, E. D., Keane, R. E. and Brown, J. K.: First Order Fire Effects Model: FOFEM 4.0, user's guide, Gen Tech Rep INT-GTR-344 Ogden UT US Dep. Agric. For. Serv. Intermt. Res. Stn. 65 P, 344, doi:10.2737/INT-GTR-344, 1997.

Schauer, J. J., Kleeman, M. J., Cass, G. R. and Simoneit, B. R. T.: Measurement of Emissions from Air Pollution Sources. 3. C1−C29 Organic Compounds from Fireplace Combustion of Wood, Environ. Sci. Technol., 35(9), 1716–1728, doi:10.1021/es001331e, 2001.

Selimovic, V., Yokelson, R. J., Warneke, C., Roberts, J. M., de Gouw, J., Reardon, J. and Griffith, D. W. T.: Aerosol optical properties and trace gas emissions by PAX and OP-FTIR for laboratory-simulated western US wildfires during FIREX, Atmos Chem Phys, 18(4), 2929–2948, doi:10.5194/acp-18-2929-2018, 2018.

Simoneit, B. R. T.: Biomass burning — a review of organic tracers for smoke from incomplete combustion, Appl. Geochem., 17(3), 129–162, doi:10.1016/S0883-2927(01)00061-0, 2002.

Simoneit, B. R. T., Schauer, J. J., Nolte, C. G., Oros, D. R., Elias, V. O., Fraser, M. P., Rogge, W. F. and Cass, G. R.: Levoglucosan, a tracer for cellulose in biomass burning and atmospheric particles, Atmos. Environ., 33(2), 173–182, doi:10.1016/S1352-2310(98)00145-9, 1999.

Spracklen, D. V., Mickley, L. J., Logan, J. A., Hudman, R. C., Yevich, R., Flannigan, M. D. and Westerling, A. L.: Impacts of climate change from 2000 to 2050 on wildfire activity and carbonaceous aerosol concentrations in the western United States, J. Geophys. Res. Atmospheres, 114(D20), D20301, doi:10.1029/2008JD010966, 2009.

Stockwell, C. E., Yokelson, R. J., Kreidenweis, S. M., Robinson, A. L., DeMott, P. J., Sullivan, R. C., Reardon, J., Ryan, K. C., Griffith, D. W. T. and Stevens, L.: Trace gas emissions from combustion of peat, crop residue, domestic biofuels, grasses, and other fuels: configuration and Fourier transform infrared (FTIR) component of the fourth Fire Lab at Missoula Experiment (FLAME-4), Atmospheric Chem. Phys., 14(18), 9727–9754, doi:https://doi.org/10.5194/acp-14-9727-2014, 2014.

Stockwell, C. E., Veres, P. R., Williams, J. and Yokelson, R. J.: Characterization of biomass burning emissions from cooking fires, peat, crop residue, and other fuels with high-resolution proton-transfer-reaction time-of-flight mass spectrometry, Atmos Chem Phys, 15(2), 845–865, doi:10.5194/acp-15-845-2015, 2015.

Stockwell, C. E., Jayarathne, T., Cochrane, M. A., Ryan, K. C., Putra, E. I., Saharjo, B. H., Nurhayati, A. D., Albar, I., Blake, D. R., Simpson, I. J., Stone, E. A. and Yokelson, R. J.: Field measurements of trace gases and aerosols emitted by peat fires in Central Kalimantan, Indonesia, during the 2015 El Niño, Atmospheric Chem. Phys., 16(18), 11711–11732, doi:https://doi.org/10.5194/acp-16-11711-2016, 2016.

Sullivan, A. P., May, A. A., Lee, T., McMeeking, G. R., Kreidenweis, S. M., Akagi, S. K., Yokelson, R. J., Urbanski, S. P., Jr, C. and L, J.: Airborne characterization of smoke marker ratios from prescribed burning, Atmospheric Chem. Phys., 14(19), 10535–10545, doi:https://doi.org/10.5194/acp-14-10535-2014, 2014.

Urbanski, S. P., Hao, W. M. and Nordgren, B.: The wildland fire emission inventory: western United States emission estimates and an evaluation of uncertainty, Atmospheric Chem. Phys., 11(24), 12973–13000, doi:https://doi.org/10.5194/acp-11-12973-2011, 2011.

Ward, D. E. and Radke, L. F.: Emissions measurements from vegetation fires: A comparative evaluation of methods and results, Crutzen P J Goldammer J G Eds Fire Environ. Ecol. Atmospheric Clim. Importance Veg. Fires Dahl. Workshop Rep. Environ. Sci. Res. Rep. 13 Chischester Engl. John Wiley Sons P 53-76, 53–76, 1993.

Westerling, A. L., Hidalgo, H. G., Cayan, D. R. and Swetnam, T. W.: Warming and Earlier Spring Increase Western U.S. Forest Wildfire Activity, Science, 313(5789), 940–943, doi:10.1126/science.1128834, 2006.

Wiedinmyer, C., Akagi, S. K., Yokelson, R. J., Emmons, L. K., Al-Saadi, J. A., Orlando, J. J. and Soja, A. J.: The Fire INventory from NCAR (FINN): a high resolution global model to estimate the emissions from open burning, Geosci Model Dev, 4(3), 625–641, doi:10.5194/gmd-4-625-2011, 2011.

Williams, B. J., Goldstein, A. H., Kreisberg, N. M. and Hering, S. V.: An in-situ instrument for speciated organic composition of atmospheric aerosols: Thermal Desorption Aerosol GC/MS-FID (TAG), Aerosol Sci. Technol., 40, 627–638, doi:10.1080/02786820600754631, 2006.

Worton, D. R., Decker, M., Isaacman-VanWertz, G., Chan, A. W. H., Wilson, K. R. and Goldstein, A. H.: Improved molecular level identification of organic compounds using comprehensive two-dimensional chromatography, dual ionization energies and high resolution mass spectrometry, Analyst, 142(13), 2395–2403, doi:10.1039/C7AN00625J, 2017.

Yokelson, R. J., Burling, I. R., Gilman, J. B., Warneke, C., Stockwell, C. E., de Gouw, J., Akagi, S. K., Urbanski, S. P., Veres, P., Roberts, J. M., Kuster, W. C., Reardon, J., Griffith, D. W. T., Johnson, T. J., Hosseini, S., Miller, J. W., Cocker III, D. R., Jung, H. and Weise, D. R.: Coupling field and laboratory measurements to estimate the emission factors of identified and unidentified trace gases for prescribed fires, Atmos Chem Phys, 13(1), 89–116, doi:10.5194/acp-13-89-2013, 2013.

Zhang, H., Yee, L. D., Lee, B. H., Curtis, M. P., Worton, D. R., Isaacman-VanWertz, G., Offenberg, J. H., Lewandowski, M., Kleindienst, T. E., Beaver, M. R., Holder, A. L., Lonneman, W. A., Docherty, K. S., Jaoui, M., Pye, H. O. T., Hu, W., Day, D. A., Campuzano-Jost, P., Jimenez, J. L., Guo, H., Weber, R. J., Gouw, J. de, Koss, A. R., Edgerton, E. S., Brune, W., Mohr, C., Lopez-Hilfiker, F. D., Lutz, A., Kreisberg, N. M., Spielman, S. R., Hering, S. V., Wilson, K. R., Thornton, J. A. and Goldstein, A. H.: Monoterpenes are the largest source of summertime organic aerosol in the southeastern United States, Proc. Natl. Acad. Sci., 115(9), 2038–2043, doi:10.1073/pnas.1717513115, 2018.

Table 1 List of fuels analyzed with the number of compounds separated and quantified from each burn. Note conifer fuel type refers to a realistic mixture of a coniferous ecosystem unless otherwise noted.

Fuel Description	Burn #	Fuel Type	Number of Compounds	MCE
Engelmann Spruce	9	Conifer	714	0.9334
Engelmann Duff	12	Coniferous Duff	751	0.859
Ponderosa Pine Rotten Log	13	Woody Debris	709	0.9778
Ponderosa Pine Litter	16	Coniferous Litter	687	0.9607
Engelmann Spruce Canopy	17	Conifer	403	0.8953
Douglas Fir Litter	22	Coniferous Litter	585	0.9501
Engelmann Spruce Duff	26	Coniferous Duff	398	0.8474
Manzanita Canopy	28	Shrub	679	0.9789
Douglas Fir Rotten Log	31	Woody Debris	776	0.7785
Manzanita Canopy	33	Shrub	570	0.9788
Engelmann Spruce Duff	36	Coniferous Duff	596	0.8773
Ponderosa Pine	37	Conifer	811	0.9403
Lodgepole Pine Canopy	40	Conifer	444	0.9231

Lodgepole Pine	42	Conifer	634	0.9524
Chamise Canopy	46	Shrub	128	0.9566
Subalpine Fir	47	Conifer	596	0.9396
Excelsior	49	Wood	173	0.9712
Yak Dung	50	Dung	515	0.9016
Peat, Kalimantan	55	Peat	392	0.8405
Subalpine Fir Duff	56	Coniferous Duff	522	0.8874
Rice Straw	60	Grass	288	0.951
Excelsior	61	Wood	230	0.9508
Bear Grass	62	Grass	656	0.9036
Lodgepole Pine	63	Conifer	834	0.938
Jeffery Pine Duff	65	Coniferous Duff	472	0.8833
Sage	66	Shrub	328	0.9191
Juniper Canopy	68	Conifer	522	0.9293
Kiln-Dried Lumber	70	Wood	209	0.953
Ceanothus Canopy	74	Shrub	97	0.9748
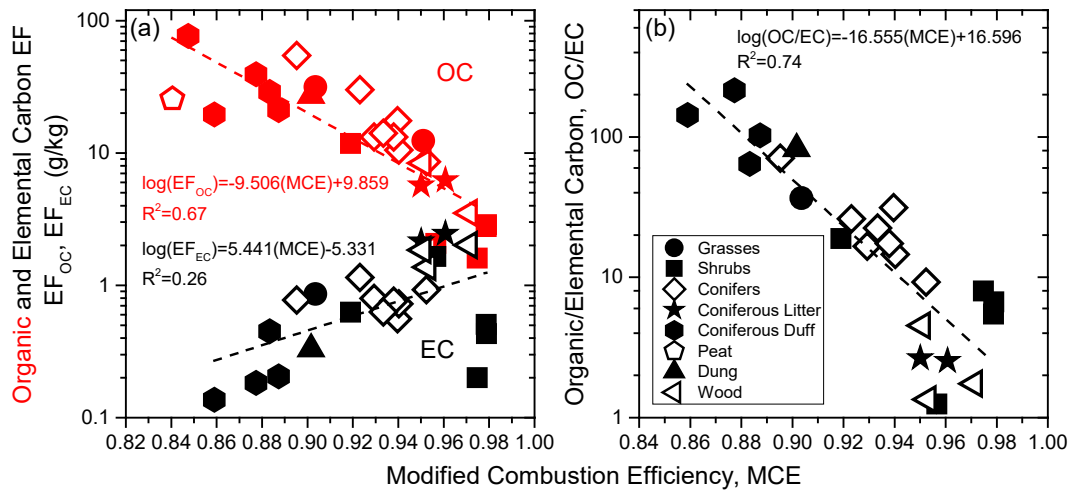
Figure 1 (a) Measured organic and elemental carbon (OC and EC, respectively) as a function of modified combustion efficiency (MCE) and (b) OC/EC as a function of MCE. Symbols indicate the different fuel types.
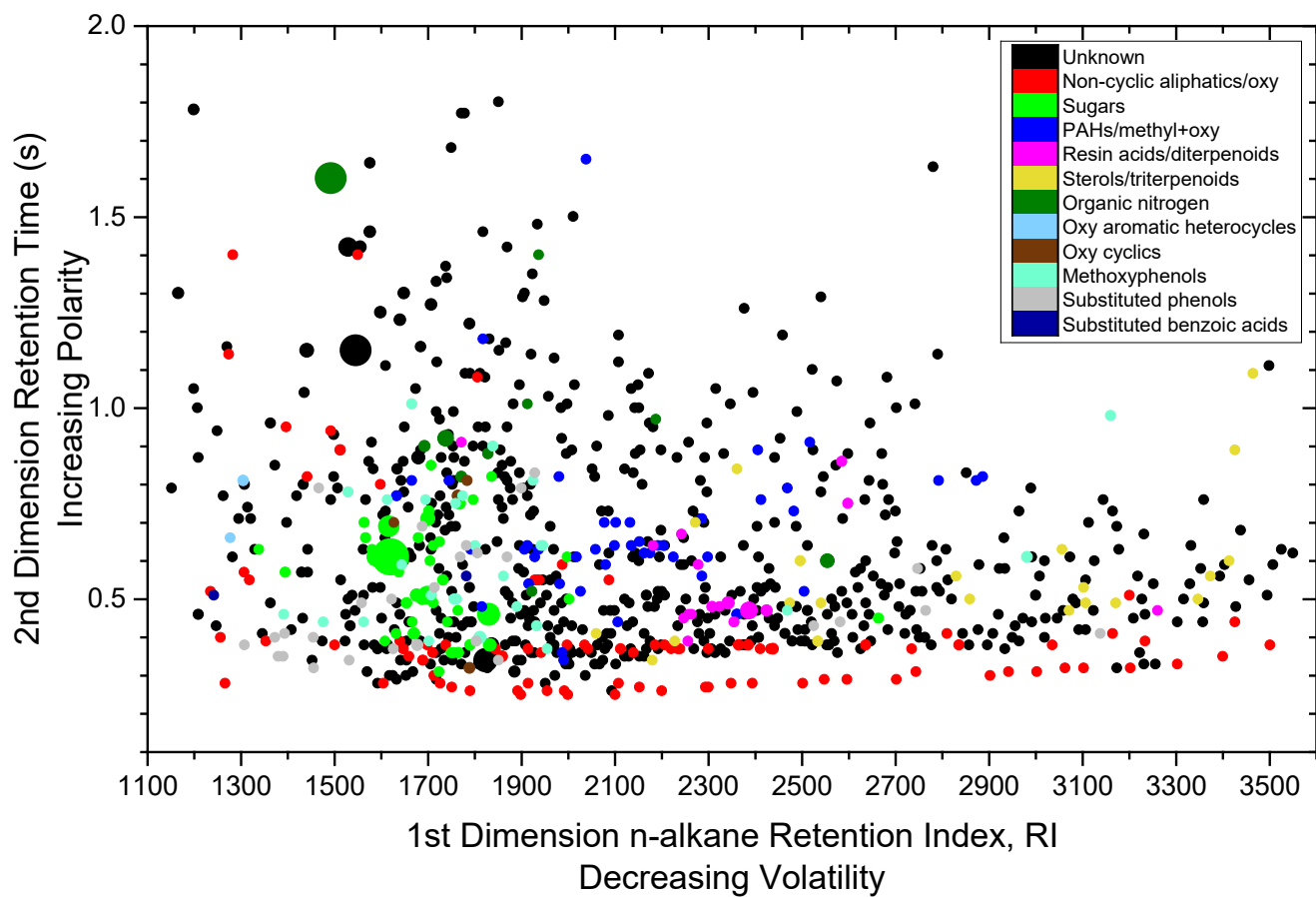
Figure 2 Two-dimensional chromatogram of smoke collected from burning lodgepole pine (burn 63). First dimension separates compounds by their volatility and second dimension by their polarity. Each point (~800 in total) represents a separated compound with the colors signifying the compound's classification. Size of a point approximately scales with its emission factor (see SI section 3).
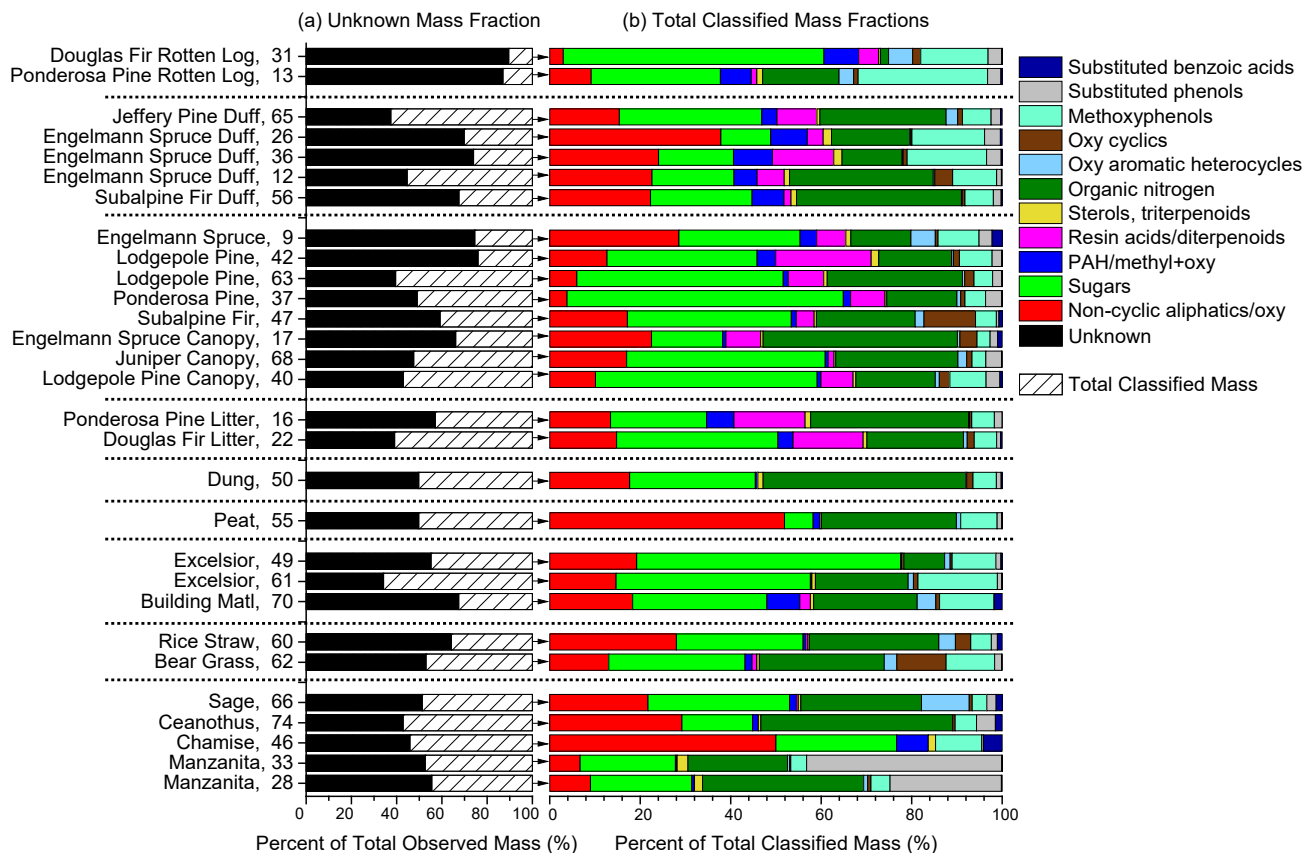
Figure 3 (a) Contributions of unknown mass to the total observed mass for the 29 analyzed burns. (b) Mass fractions for each chemical family compared to total classified mass. Fuels are grouped by type and numbers after fuel name indicate the burn number during the FIREX campaign.

Figure 4 Summed emission factors (EFs) within a chemical family for each burn as a function of modified combustion efficiency (MCE). Each panel depicts a different family with (a) total observed I/SVOC EF, (b) unknowns, (c), sugars, (d) Polycyclic aromatic hydrocarbons (PAHs, including methylated and oxygenated forms), (e) methoxyphenols, and (f) sterols/triterpenoids. Dashed lines represent a log fit of the form log(EF) inversely proportional to MCE. The dotted lines represented a factor of 2 above and below the model. Symbols denote different fuel types.

Figure 5 Emission factors (EFs) of (a) levoglucosan (sugar), (b) fluoranthene (PAH), (c) acetovanillone (methoxyphenol), (d) coniferyl aldehyde (methoxyphenol) for various fuel burns as a function of MCE. Dashed lines indicate a log fit of the form log(EF) inversely proportional to MCE. Dotted lines show a factor of 2 above and below the model. Note, peat (open pentagon) is not included in any of the fits. Different symbols represent fuel categories.

Speciated and total emission factors of particulate organics from burning western U.S. wildland fuels and their dependence on combustion efficiency

Coty N. Jen[1,6], Lindsay E. Hatch[2], Vanessa Selimovic[3], Robert J. Yokelson[3], Robert Weber[1], Arantza E. Fernandez[4], Nathan M. Kreisberg[4], Kelley C. Barsanti[2], Allen H. Goldstein[1,5]

[1] Department of Environmental Science, Policy, and Management, University of California, Berkeley, Berkeley, CA, 94720 USA

[2] Department of Chemical and Environmental Engineering and College of Engineering – Center for Environmental Research and Technology, University of California, Riverside, Riverside, CA, 92507, USA

[3] Department of Chemistry, University of Montana, Missoula, 59812, USA

[4] Aerosol Dynamics Inc., Berkeley, CA 94710, USA

[5] Department of Civil and Environmental Engineering, University of California, Berkeley, Berkeley, CA 94720, USA

[6] now at Department of Chemical Engineering, Carnegie Mellon University, Pittsburgh, PA 15213, USA

Supporting Information:

1. **Sampling position and diagram of DEFCON, Direct Emission Fire CONcentrator**
2. **I/SVOCs from the FIREX FSL experiments-- University of California, Berkeley-Goldstein Library of Biogenic and Environmental Spectra (UCB-GLOBES)**
3. **Conversion of instrument response to mass loadings and emission factors**
4. **Internal/external standards and mass loading calibration curves**
5. **Classifying unidentified compounds into chemical families**
6. **Classified I/SVOC mass fractions averaged over fuel type**
7. **EFs for families of compounds as a function of MCE**

1. Sampling position and diagram of DEFCON, Direct Emission Fire CONcentrator:

Smoke was collected directly from the stack at a position ~17 m above the burn (Figure S1). A flow of 10.3 LPM was pulled through DEFCON. 300 sccm of the flow was diverted to two parallel absorbent tube sampling channels (150 sccm each channel). The reminder of the smoke flow (10 LPM) was then passed through a 1.0 μm cyclone prior to collection on a 10 cm quartz fiber filter. Flow rates were continuously monitored to ensure correct flows. All metal surfaces except for the cyclone and filter holders were passivated with Inertium® to minimize loss of oxygenated organics (Williams et al., 2006). A diagram of DEFCON is given in Figure S2.
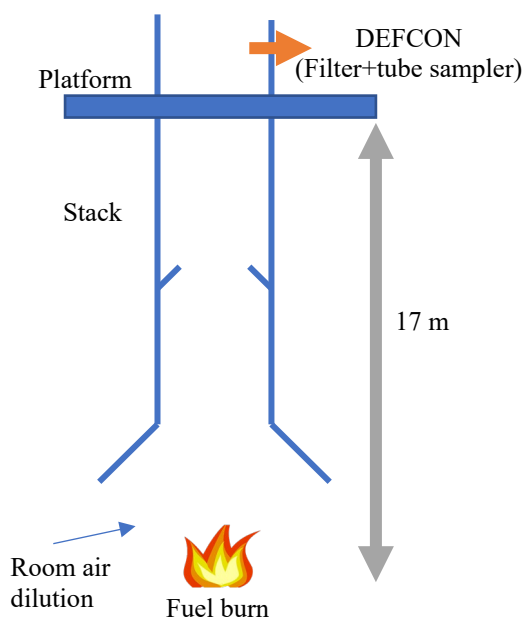
Figure S1 Diagram of the smoke stack in the burn room and the placement of DEFCON
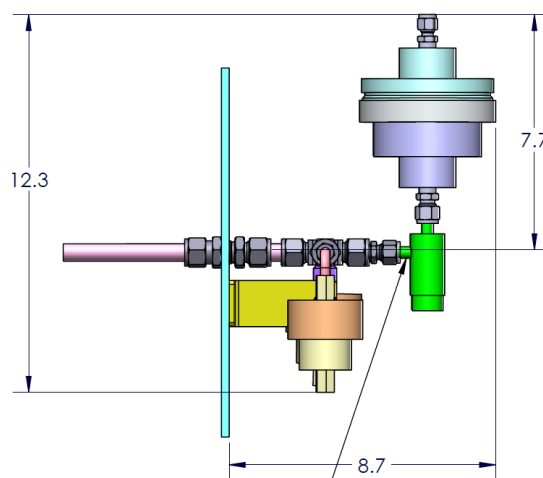
Figure S2 Schematic of DEFCON and how it sampled from the stack

2. I/SVOCs from the FIREX FSL experiments-- University of California, Berkeley-Goldstein Library of Organic Biogenic and Environmental Spectra (UCB-GLOBES):

The mass spectrum and retention index of each compound separated by the TD-GC×GC-EI/VUV-HRToFMS was compared to the NIST mass spectral database (2014 version) and/or to previous literature. Table S1 provides a list of all 149 identified compounds and its identification method. In addition, all separated and unique compounds from the 29 analyzed burns were compiled into UCB-GLOBES (FIREX), https://nature.berkeley.edu/ahg/data/MSLibrary/. Information includes compound chemical classification, deuterated and non-deuterated *n*-alkane retention indices, mass spectrum, instrument/method details, derivatization agent, list of fuel, and, if found in 10 or more burns, the slope, intercept, standard errors, and R^2 for the model log(EF)=slope(MCE)+int. UCB-GLOBES (FIREX) is NIST MS Search compatible and can be used in the future to better identify biomass-burning derived organic compounds found in the atmosphere.

Table S1 *List of identified compounds and their sources, characteristic EI ions and retention index (RI). Compounds were identified using a combination of RI, mass spectrum, VUV parent ion mass, or standard matching.*

Compound name	Underiv. Formula	Derivatized Formula	Exact Mass (no deriv)	Exact Mass (Deriv)	Top 5 masses (deriv)	RI	ID Method	Comments
Glycerol 3TMS	C3H8O3	C12H32O3Si3	92.047	308.166	69, 73, 147, 131, 205	1266	RI, MS, VUV	All forms of pine, dung, rice straw, sage
Glyceric acid 3TMS	C3H6O4	C12H30O4Si3	106.027	322.145	73, 147, 189, 133, 117	1319	RT, MS, VUV	Rotten log
Catechol 2TMS	C6H6O2	C12H22O2Si2	110.037	254.116	73, 254, 239, 45, 74	1307	RT, MS, VUV, STD	All
Hydroquinone 2 TMS	C6H6O2	C12H22O2Si2	110.037	254.116	239, 254, 73, 240, 255	1393	RT, MS, VUV, STD	All
Resorcinol 2TMS	C6H6O2	C12H22O2Si2	110.037	254.116	239, 254, 73, 69, 91	1372	RT, MS, VUV, STD	All forms of pine, ground, manzanita, juniper
1,2-cyclohexanediol	C6H12O2	C12H28O2Si2	116.084	260.162	'147, 73, 142, 81, 245'	1253	RT, MS, VUV	Duff
Butanedioic acid 2TMS	C4H6O4	C10H22O4Si2	118.027	262.106	147, 73, 75, 148, 45	1306	RI, MS, VUV	All
3-methylcatechol 2TMS	C7H8O2	C13H24O2Si2	124.052	268.131	73, 268, 74, 45, 253	1379	RI, MS, VUV	All
4-methylcatechol 2TMS	C7H8O2	C13H24O2Si2	124.052	268.131	73, 69, 268, 253, 45	1390	RT, MS, VUV, STD	All
Benzoic acid TMS steroisomer 1	C7H8O2	C10H16O2Si	124.052	196.092	105, 179, 135, 77, 194	1242	RI, MS, VUV	All
Benzoic Acid TMS steroisomer 2	C7H8O2	C10H16O2Si	124.052	196.092	105, 179, 135, 77, 194	1234	RI, MS, VUV	All
Methylhydroquinone 2TMS	C7H8O2	C13H24O2Si2	124.052	268.131	268, 253, 73, 237, 254	1454	RI, MS, VUV	All
5-(hydroxymethyl) furfural TMS	C6H6O3	C9H14O3Si	126.032	198.071	183, 109, 111, 73, 81	1304	RI, MS, VUV	All
Maltol TMS	C6H6O3	C9H14O3Si	126.032	198.071	183, 184, 153, 75, 111	1277	RT, MS, VUV, STD	All
Pyrogallol 3TMS	C6H6O3	C15H30O3Si3	126.032	342.150	239, 73, 342, 240, 211	1531	RT, MS, VUV	All
Pyroglutamic acid TMS	C5H7NO3	C11H23NO3Si2	129.043	273.122	84, 75, 73, 41, 45	1492	RT, MS, VUV, STD	All
Methylsuccinic acid 2TMS	C5H8O4	C11H24O4Si2	132.042	276.121	73, 147, 217	1317	RT, MS, VUV	All forms of pine, bear grass, dung, manzanita

3-hydroxyacetophenone TMS	C8H8O2	C11H16O2Si	136.052	208.092	193, 73, 208, 43, 75	1466	RI, MS, VUV	All
3-Hydroxybenzoic acid 2 TMS	C7H6O3	C13H22O3Si2	138.032	282.111	267, 223, 193, 73, 282	1558	RI, MS, VUV	All
4-Hydroxybenzoic acid 2TMS	C7H6O3	C13H22O3Si2	138.032	282.111	267, 223, 73, 193, 268	1622	RI, MS, VUV	All
1-4:3-6-Dianhydro-alpha-d-glucopyranose TMS	C6H8O4	C9H16O4Si	144.042	216.081	73, 129, 75, 155, 170	1338	RI, MS, VUV	All
Arabinonic acid, 1,4-lactone 3TMS	C5H8O5	C14H32O5Si3	148.037	364.156	73, 147, 117, 75, 217	1627	RI, MS, VUV	All pine forms, bear grass, manzanita
P-Coumaric alcohol 2TMS	C9H10O2	C15H26O2Si2	150.068	294.147	73, 205, 294	1625	RI, MS, VUV	All forms of pine and juniper
2, 4-dihydroxyacetophenone 2TMS	C8H8O3	C14H24O3Si2	152.047	296.126	217, 73, 281, 218, 75	1688	RI, MS, VUV	All forms of pine
Vanillin TMS	C8H8O3	C11H16O3Si	152.047	224.087	194, 193, 209, 73, 195	1529	RT, MS, VUV, STD	All forms of pine, peat, juniper
Arabinitol 5TMS	C5H12O5	C20H52O5Si5	152.068	512.266	73, 217, 147, 103, 205	1713	RI, MS	All pine forms except rotten log
Protocatechoic acid 3TMS	C7H6O4	C16H30O4Si3	154.027	370.145	193, 73, 370, 355, 311	1812	RT, MS, VUV	All forms of pine, peat, sage, juniper
Syringol TMS	C8H10O3	C11H18O3Si	154.063	226.103	196, 211, 181, 69, 197	1391	RT, MS, VUV, STD	All
4-nitrocatechol 2TMS	C6H5NO4	C12H21NO4Si2	155.022	299.101	73, 284, 299, 45, 74	1738	RI, MS, VUV, STD	All
Nonanoic acid TMS	C9H18O2	C12H26O2Si	158.131	230.170	69, 75, 131, 73, 117	1353	RT, MS, VUV, STD	All
1-8-dihydroxynaphthalene 2TMS	C10H8O2	C16H24O2Si2	160.052	304.131	73, 304, 217, 45, 74	1815	RI, MS, VUV	All
Umbelliferone TMS	C9H6O3	C12H14O3Si	162.032	234.071	219, 234, 73, 220, 191	1818	RT, MS, VUV	All forms of pine, dung, manzanita, grasses, sage, juniper
Deoxy-ribo-hexonic acid 1-4-lactone 3 TMS	C6H10O5	C15H34O5Si3	162.053	378.171	73, 147, 129, 155, 103	1764	RI, MS	All
Galactosan 3TMS	C6H10O5	C15H34O5Si3	162.053	378.171	217, 73, 204, 218, 147	1654	RT, MS, VUV, STD	All

Levoglucosan 3 TMS	C6H10O5	C15H34O5Si3	162.053	378.171	73, 204, 217, 147, 189	1698	RT, MS, VUV, STD	All
Mannosan 3TMS	C6H10O5	C15H34O5Si3	162.053	378.171	73, 217, 204, 191, 147	1676	RI, MS	All forms of pine
4-Coumaric acid 2TMS	C9H8O3	C15H24O3Si2	164.047	308.126	293, 219, 73, 249, 308	1934	RI, MS, VUV	All
Eugenol TMS	C10H12O2	C13H20O2Si	164.084	236.123	206, 221, 236, 179, 73	1464	RT, MS, VUV	Engelmann spruce duff
4-vinylveratrole	C10H12O2		164.084		164, 149, 91, 77, 121	1358	RT, MS, VUV	Duff
Isoeugenol TMS	C10H12O2	C13H20O2Si	164.084	236.123	206, 205, 236, 207, 69	1562	RI, MS, VUV	All forms of pine, dung, grasses, juniper
Acetovanillone TMS	C9H10O3	C12H18O3Si	166.063	238.103	193, 223, 208, 73, 238	1612	RI, MS, VUV	All
Phloretic acid 2TMS	C9H10O3	C15H26O3Si2	166.063	310.142	179, 73, 180, 75, 45	1806	RT, MS, VUV	Bear grass, pine, manzanita
3-(Methylthio)benzoic acid TMS	C8H8O2S	C11H16O2SSi	168.025	240.064	225, 181, 151, 240, 75	1640	RI, MS, VUV	Rotten log
Methyl 3,4-dihydroxybenzoate 2TMS	C8H8O4	C14H24O4Si2	168.042	312.121	193, 73, 312, 194, 45	1714	RI, MS, VUV	All forms of pine
Vanillic acid 2TMS	C8H8O4	C14H24O4Si2	168.042	312.121	297, 267, 223, 253, 282	1755	RT, MS, VUV, STD	All
1-acenaphthenone	C12H8O		168.058		140, 168, 139, 73, 89	1665	RI, MS, VUV	Pine, sage, juniper
Homovanillyl alcohol 2TMS	C9H12O3	C15H28O3Si2	168.079	312.158	209, 73, 312, 210, 179	1702	RT, MS, VUV	All
Methylsyringol TMS	C9H12O3	C12H20O3Si	168.079	240.118	210, 69, 211, 225, 240	1476	RT, MS, VUV	All
Methyl nitrocatechol 2 TMS isomer 1	C7H7NO4	C10H15NO4Si	169.038	241.077	73, 296, 45, 313, 180	1771	RI, MS, VUV	All
Methyl nitrocatechol 2 TMS isomer 2	C7H7NO4	C10H15NO4Si	169.038	241.077	73, 298, 75, 45, 74	1828	RI, MS, VUV	All
Gallic acid 4TMS	C7H6O5	C19H38O5Si4	170.022	458.180	281, 73, 443, 458, 179	1947	RI, MS, VUV	Manzanita

Name	Formula	TMS Formula	Mass	TMS Mass	Fragments	RI	Methods	Source
1,4-Dihydroxy-2,6-dimethoxybenzene 2TMS	C8H10O4	C14H26O4Si2	170.058	314.137	284, 314, 73, 299, 269	1669	RI, MS, VUV	All
4-phenylphenol TMS	C12H10O	C15H18OSi	170.073	242.113	211, 227, 73, 242, 310	1771	RI, MS, VUV	All
Shikimic acid 4TMS	C7H10O5	C19H42O5Si4	174.053	462.211	204, 73, 147, 205, 206	1803	RT, MS, VUV	Pine and pine litter
Esculetin 2 TMS	C9H6O4	C15H22O4Si2	178.027	322.106	73, 322, 307, 45	2093	RT, MS, VUV	Sage
Coniferyl aldehyde TMS	C10H10O3	C13H18O3Si	178.063	250.103	220, 219, 250, 192, 73	1839	RT, MS, VUV	All
Phenanthrene	C14H10		178.078		178, 73, 176, 152, 177	1791	RT, MS, VUV, STD	All
9-fluorenone	C13H8O		180.058		180, 152, 151, 181, 150	1745	RI, MS, VUV	All
Benzocinnoline	C12H8N2		180.069		152, 180, 151, 76, 150	1913	RI, MS, VUV	All
Coniferyl alcohol 2TMS	C10H12O3	C16H28O3Si2	180.079	324.158	219, 193, 73, 309, 220	1946	RI, MS, VUV	Pine and juniper
Homovanillic acid 2TMS	C9H10O4	C15H26O4Si2	182.058	326.137	73, 209, 179, 267, 326	1761	RI, MS, VUV	All
Syringaldehyde TMS	C9H10O4	C12H18O4Si	182.058	254.097	73, 204, 217, 224, 147	1695	RT, MS, VUV, STD	Pine and manzanita
Dihydroconiferyl alcohol 2TMS	C10H14O3	C16H30O3Si2	182.094	326.173	206, 205, 236, 73, 326	1811	RI, MS, VUV	All
6H-Cyclobuta[jk]phenanthrene	C15H10		190.078		190, 189, 95, 191, 187	1928	RI, MS, VUV	Pine, shrubs, bear grass
Scopoletin TMS	C10H8O4	C13H16O4Si	192.042	264.082	234, 206, 264, 73, 249	2031	RT, MS, VUV	Sage, rotten log, duff
Quinic acid 5TMS	C7H12O6	C22H52O6Si5	192.063	552.261	73, 345, 255, 147, 69	1851	RT, MS, VUV	Pine, manzanita, sage
9-methylanthracene	C15H12		192.094		192, 191, 189, 190, 165	1936	RI, MS, VUV	All
Methylanthracene isomer	C15H12		192.094		192, 191, 189, 190, 193	1906	RI, MS, VUV	All forms of pine, dung, bear grass, sage
1-methylanthracene	C15H12		192.094		192, 191, 189, 190, 193	1912	RI, MS, VUV	All

Methyl caffeate 2TMS	C10H10O4	C16H26O4Si2	194.058	338.137	73, 323, 249, 308, 338	2087	RI, MS, VUV	All forms of pine, ground, grasses, juniper
Pinitol 5TMS	C7H14O6	C22H54O6Si5	194.079	554.277	73, 217, 247, 147, 159	1788	RT, MS, VUV, STD	Pine and pine litter
Naphthalic anhydride	C12H6O3		198.032		154, 126, 198, 63, 50	2038	RI, MS, VUV	Pine and juniper
D-Arabino Hexonic acid 3-deoxy-2,5,6-tris-O-(TMS)-lactone	C9H10O5	C18H34O5Si3	198.053	414.171	73, 147, 129, 103, 75	1783	RI, MS	All
Syringic acid 2TMS	C9H10O5	C15H26O5Si2	198.053	342.132	73, 75, 312, 159, 297	1890	RT, MS, VUV, STD	All forms of pine, ground, manzanita, juniper
β-Carboline, 7-hydroxy-1-methyl TMS	C12H10ON2	C15H18N2OSi	198.079	270.119	255, 270, 73, 240, 75	1922	RT, MS, VUV	All forms of pine, juniper
Vanillyl glycol 3TMS	C10H14O4	C19H38O4Si3	198.089	414.208	73, 147, 117, 205, 209	1955	RT, MS, VUV	All forms of pine and juniper
Fluoranthene	C16H10		202.078		202, 203, 200, 201, 101	2077	RT, MS, VUV, STD	All
Pyrene	C16H10		202.078		202, 200, 203, 201, 101	2132	RT, MS, VUV, STD	All
Acephenanthrene	C16H12		204.094		202, 200, 203, 201, 101	2101	RT, MS, VUV	All
Pimanthrene	C16H14		206.110		206, 191, 204, 205, 189	2058	RT, MS, VUV	All
Anthraquinone	C14H8O2		208.052		208, 152, 180, 76, 151	1980	RT, MS, VUV, STD	Sage, lodgepole pine forms
Ethyl homovanillate TMS	C11H19O4	C14H27O4Si	215.128	287.168	252, 179, 209, 73, 282	1771	RT, MS, VUV	Pine litter, duff, rotten log, dung, and grasses
Benzofluorene	C17H12		216.094		216	2109	RT, MS, VUV	All forms of pine and shrubs
Octanoic acid TMS	C8H16O2	C11H24O2Si	216.155	144.115	73, 75, 117, 201, 131	1255	RT, MS, VUV, STD	All
2, 3-5, 6-dibenzoxalene	C16H10O		218.073		218, 73, 189, 91, 219	2191	RI, MS, VUV	Lodgepole
Benzo[b]naphtho[1,2-d]furan	C16H10O		218.073		218, 189, 219, 204	2135	RT, MS, VUV	Pine, manzanita, sage, bear grass
Benzo[kl]xanthene	C16H10O		218.073		218, 202, 217, 203, 219	2203	RT, MS, VUV	All pine forms
Hydroxypyrene	C16H10O	C19H18OSi	218.073	290.113	218, 189, 73, 219, 95	2152	RT, MS, VUV	Lodgepole pine

Compound	Formula	TMS Formula	Mass	TMS Mass	Ions	RI	Methods	Sources
Vanillic acid isobutyl ester TMS	C12H16O4	C15H24O4Si	224.105	296.144	241, 256, 225, 73, 242	1861	RT, MS, VUV	All forms of pine, peat, manzanita
Cyclopenta[cd]pyrene	C18H10		226.078		226, 224, 227, 113, 225	2468	RT, MS, VUV	Pine, shrubs, bear grass
9-Tetradecenoic acid TMS	C14H26O2	C17H34O2Si	226.193	298.233	73, 75, 117, 283, 129	1836	RT, MS, VUV	Bear grass, duff, pine
Chrysene	C18H12		228.094		228, 226, 229, 114, 227	2482	RT, MS, VUV, STD	Pine, shrubs, bear grass
Benzanthrone	C17H10O		230.073		230, 202, 101, 200	2516	RT, MS, VUV	Lodgepole, pine, and manzanita
B-Cyclocostunolide	C15H20O2		232.146		217, 232, 91	1928	RT, VUV	sage, juniper
1-(10-Methylanthracen-9-yl)ethanone	C17H14O		234.104		219, 191, 189, 234, 190	2405	RT, MS, VUV	All forms of pine
Retene	C18H18		234.141		219, 234, 204, 203, 220	2225	RT, MS, VUV, STD	All
Ethylhexyl benzoate	C15H22O2		234.162		105, 70, 77, 112, 83	1707	RT, MS, VUV, STD	All forms of pine and shrubs
Heptadecane (C17)	C17H36		240.282		57, 71, 43, 131	1698	RT, MS, VUV, STD	Dung, peat, rice straw, and pine bark
Confertin	C15H20O3		248.141		248, 81, 119	2043	RT, MS, VUV	Sage
Benzo[a]pyrene	C20H12		252.094		252, 250, 253, 126, 113	2886	RT, MS, VUV, STD	Pine, sage, juniper
Benzofluoranthene isomer 1	C20H12		252.094		252, 253, 250, 125, 126	2792	RT, MS, VUV, STD	Pine, sage, juniper, manzanita
Benzofluoranthene isomer 2	C20H12		252.094		252, 250, 253, 73, 126	2873	RT, MS, VUV, STD	Pine, juniper
11-Hexadecenoic acid TMS	C16H30O2	C19H38O2Si	254.225	326.264	55, 69, 83, 41, 96	1938	RT, MS, VUV	All
Palmitic acid TMS	C16H32O2	C19H40O2Si	256.240	328.280	117, 73, 313, 75, 129	2042	RT, MS, VUV, STD	All
Nonadecane (C19)	C19H40		268.313		57, 71, 43, 131	1897	RT, MS, VUV, STD	All
Heptadecanoic acid TMS	C17H34O2	C20H42O2Si	270.256	342.295	73, 117, 75, 129, 327	2112	RT, MS, VUV, STD	All forms of pine, dung, peat, and bear grass
Methyl 13-methylpentadecanoate	C17H34O2		270.256		74, 87, 270	1922	RT, VUV	Pine, ground, and grass
Arbutin 4TMS	C12H16O7	C24H48O7Si4	272.090	560.248	73, 182, 254, 129, 103	2563	RT, MS	Manzanita

Divanillyl 2TMS	C16H18O4	C22H34O4Si2	274.120509	418.2009	209, 73, 210, 179, 211	2468	RT, MS, VUV	All forms of pine, dung, juniper
Dibutyl phthalate	C16H22O4		278.152		149, 57	1857	MS, VUV	All
Linoelaidic acid TMS	C18H32O2	C21H40O2Si	280.240	352.280	75, 73, 67, 81, 95	2206	RT, MS, VUV	All
Oleic acid TMS	C18H34O2	C21H42O2Si	282.256	354.295	73, 75, 117, 129, 55	2220	RT, MS, VUV	All
Icosane (C20)	C20H42		282.329		57, 131, 71, 85	1998	RT, MS, VUV, STD	All
Dehydroabietal	C20H28O		284.214		159, 269, 173, 209, 241	2278	RT, MS, VUV	All forms of pine
Stearic acid TMS	C18H36O2	C21H44O2Si	284.272	356.311	117, 73, 75, 341, 129	2238	RT, MS, VUV, STD	All
Isopimaral	C20H30O		286.230		187, 131, 105, 91, 145	2241	RT, MS, VUV	Pine and pine litter
Henicosane (C21)	C21H44		296.344		57, 131, 71, 43	2100	RT, MS, VUV, STD	All
18-Methyl-nonadecanol TMS	C20H42O	C23H50OSi	298.324	370.363	75, 355, 97, 73, 69	2348	RI, MS, VUV	All forms of pine, grass, sage
Dehydroabietic acid TMS	C20H28O2	C23H36O2Si	300.209	372.248	239, 240, 73, 173, 357	2386	RT, MS, VUV	All
Abietic acid TMS	C20H30O2	C23H38O2Si	302.225	374.264	256, 241, 185, 213, 73	2424	RT, MS, VUV, STD	Pine and bear grass
Isopimaric Acid TMS	C20H30O2	C23H38O2Si	302.225	374.264	241, 73, 242, 359, 105	2354	RT, MS, VUV, STD	All forms of pine
Isopimaric acid TMS isomer	C20H30O2	C23H38O2Si	302.225	374.264	241, 256, 73, 257, 242	2342	RT, MS, VUV, STD	All forms of pine and bear grass
Pimaric acid TMS	C20H30O2	C23H38O2Si	302.225	374.264	121, 73, 120, 257, 91	2307	RT, MS, VUV	All forms of pine and bear grass
Sandaracopimaric acid TMS	C20H30O2	C23H38O2Si	302.225	374.264	73, 121, 120, 119, 81	2323	RT, MS, VUV	All forms of pine and juniper
Docosane (C22)	C22H46		310.360		57, 71, 43, 131	2199	RT, MS, VUV, STD	Pine and grass
Hexadecanoic acid, 3,7,11,15-tetramethyl TMS	C20H40O2	C23H48O2Si	312.303	384.342	117, 73, 75, 369, 129	2438	RT, MS, VUV	All
7-Oxo-dehydroabietic acid TMS	C20H26O3	C23H34O3Si	314.188	386.228	253, 268, 73, 187, 386	2598	RI, MS, VUV	Pine and bear grass

Tricosane (C23)	C23H48		324.376		57, 71, 43, 85	2299	RT, MS, VUV, STD	All
7-Oxodehydroabietic acid methyl ester	C21H28O3		328.204		253, 254, 187, 211, 328	2585	RI, MS, VUV	All forms of pine
Tetracosane (C24)	C24H50		338.391		57, 97, 83, 55	2393	RT, MS, VUV, STD	All
3,4-divanillyltetrahydrofuran 2TMS	C20H24O5	C26H40O5Si2	344.162	488.241	209, 210, 73, 179, 488	2981	RT, MS, VUV	All
Pentacosene	C25H50		350.391		83, 57, 97, 43	2494	RT, VUV	Ground, manzanita, bear grass
Pentacosane (C25)	C25H52		352.407		57, 71, 131, 85	2501	RT, MS, VUV, STD	All
1-tetracosanol (C24 Alcohol)	C24H50O	C27H58OSi	354.386	426.426	75, 411, 97, 57, 412	2743	RT, MS, VUV, STD	All
Matairesinol 2TMS	C20H22O6	C26H38O6Si2	358.142	502.221	209, 73, 179, 210, 502	3160	RT, MS, VUV	Pine, pine litter, and juniper
Hexacosene	C26H52		364.407		57, 69, 97, 111, 83	2595	RT, MS, VUV, STD	Ground, manzanita, bear grass
Hexacosane (C26)	C26H54		366.423		131, 57, 83, 55	2595	RT, MS, VUV, STD	Pine, ground, and grass
Heptacosane (C27)	C27H56		380.438		57, 71, 85, 69, 43	2701	RT, MS, VUV, STD	All
Stigmasta-3,5 diene	C29H48		396.376		147, 81, 145, 105, 91	3106	RT, MS, VUV	All
Nonacosane (C29)	C29H60		408.470		57, 71, 85, 43, 69	2901	RT, MS, VUV, STD	All
β-sitosterol TMS	C29H50O	C32H58OSi	414.386	486.426	129, 73, 75, 95, 121	3347	RT, MS, VUV, STD	All
10-nonacosanol TMS	C29H60O	C32H68OSi	424.464	496.504	229, 73, 75, 369, 83	3062	RT, MS, VUV, STD	All forms of pine, juniper
Tocopherol TMS	C29H50O2	C32H58O2Si	430.381	502.421	237, 73, 236, 502, 238	3138	RT, MS, VUV	All
Triacontane (C30)	C30H62		436.501		57, 71, 85, 43	3001	RT, MS, VUV, STD	All
Hentriacontane (C31)	C31H64		464.532		57, 71, 85, 69, 43	3102	RT, MS, VUV, STD	All
Dotriacontane (C32)	C32H66		492.563		57, 71, 85, 131	3202	RT, MS, VUV, STD	All

Tritriacontane (C33)	C33H68		520.595		57, 71, 69, 43, 85	3302	RT, MS, VUV, STD	All
Tetratriacontane (C34)	C34H70		548.626		57, 71, 85, 131	3399	RT, MS, VUV, STD	All
Pentatriacontane (C35)	C35H72		576.657		71, 57, 85, 131	3500	RT, MS, VUV, STD	All

3. Conversion of instrument response to mass loadings and emission factors:

Internal standard was injected onto each sample filter prior to analysis on the TD-GC×GC-EI/VUV-HRToFMS. This was done to correct for matrix effects and slight changes in instrument performance. The internal standard mixture consisted of relevant biomass burning deuterated compounds (see next section). The total volume of each chromatographic peak was integrated and normalized to the nearest internal standard peak volume. The normalized peak volume was then converted to mass loading by finding the nearest standard compound of the same compound class in first and second dimension and using its accompanying mass loadings calibration curve (see next section for more details). In other words, compounds classified as sugars were converted to mass loadings based upon the calibration of the nearest sugar standard. Unknown compounds were matched to the nearest standard compound regardless of chemical classification.

Mass loading calibration curves were determined by measuring the instrument's response to varying amounts of 99 standard compounds typically found in biomass burning organic aerosol particles. We estimate the systematic uncertainty in the mass loadings for the unknown compounds at a factor of 2. Unidentified but classified compounds exhibited lower uncertainty due to similarities in instrument response to standards within the same family. To illustrate this reduction of uncertainty, we examine compounds with a RI of in the range of 1800-1900. Compounds that elute in this region include sugars, PAHs, aliphatics, and organic nitrogen. Their associated slopes from their mass loading calibration curves and compound family are provided in Table S2. Slopes within compound families are more similar than between families. For example, sugars exhibit slopes on average of 0.19 (not all shown in Table S2) whereas aliphatics have slopes of 1.1. An unclassified sample compound that elutes near myristic acid and galactose could be converted to mass loadings using either the slopes of myristic acid (0.43) or galactose (0.004). Depending which is chosen, the estimated mass loading of this unclassified compounds could range over three orders of magnitude. However, if this sample compound were classified as a sugar, then the estimated mass loadings would be significantly higher and more in-line with the how typical sugars respond in the instrument. Our observations using various standard compounds indicate this calibration technique primarily lowers the uncertainty of more polar compounds to ±~30%.

Table S2 Example mass loading calibrations slopes for compounds in the RI=1800 range.

Compound Name	1D RI	2D retention time (s)	Mass Calibration Slopes	Compound Family
Octadecane (C18)	1831	0.260	1.70	Aliphatic
Mannose	1831	0.310	0.19	Sugar
Anthracene	1836	0.680	1.82	PAHs
Pinitol	1856	0.330	0.37	Sugar
5-Nitrovanillin	1866	1.350	0.67	Organic nitrogen
Myristic Acid (C14 acid)	1879	0.380	0.43	Aliphatic
Galactose	1885	0.320	0.004	Sugar

Sampled compounds that exactly matched a standard compound have a lower uncertainty of ~±10% that is primarily due to instrument variation. Since the same data inversion factor was applied to the same observed compound across all samples, these systematic uncertainties do not affect the trends observed in this study but may affect the mass fractions each compound contributes to the total observed mass from a burn.

The background-subtracted compound mass loading was then converted to emission factors by first normalizing to the background-corrected CO_2 mass sampled. CO_2 concentration (by volume) was measured in real-time by the open-path Fourier transform infrared spectroscopy (OP-FTIR). Details of this measurement can be found in Selimovic et al. (2018). The mass of CO_2 that pass through a filter was calculated by first converting the CO_2 volume concentration into mass concentration. CO_2 mass concentration was then numerically integrated over the filter sampling time then multiplied by the total volumetric flow through the filter. The normalized organic compound mass loadings were converted to emission factors, $EF_{compound}$, via the fire-integrated EF_{CO2} following the formula below (units are given in parentheses).

$$EF_{compound} = \frac{\Delta mass\ of\ compound\ (ng)}{\Delta mass\ of\ CO_2\ (g)} \times EF_{CO2}\ (g/kg\ dry\ fuel\ burned)$$

The Δ indicate change over background. EFs_{CO2} for each burn during FIREX Fire Lab campaign are also presented Selimovic et al. (2018) and were determined by the carbon mass balance method (Ward and Radke, 1993; Yokelson et al., 1996). The carbon mass was summed over the gaseous species detected by the OP-FTIR, with CO_2, CO, and CH_4 accounting for 97-99% of the total emitted carbon. Including the carbon mass of the I/SVOCs would only slightly decrease the EFs reported here and thus their contributions to the carbon mass balance were assumed to be negligible.

EFs for all observed compounds are provided in the open access FIREX data archive (see Data Sets of the main paper). Figure 2 illustrates the EFs for the observed compounds from a lodgepole pine burn. The marker sizes approximately scale with EFs. However, corrections were made to the floor and ceiling limits of the marker sizes. This was done to prevent some markers from dominating the entire area of the chromatogram and the minute points from fading from view.

4. **Internal/external standards and mass loading calibration curves:**

A mixture of deuterated internal standards was injected onto every filter prior to analysis. The mixture consisted of 34 compounds that are either found in biomass burning organic aerosols (BBOA) or have functional groups that closely resemble compounds in BBOA. A full list of internal standard compounds is given in Table S3.

A more extensive mixture of standards was used to calibrate the mass loading sensitivity of the TD-GC×GC EI-HRToFMS directly after all the Fire Lab samples were run. This mixture of external standards contained 99 compounds that have been previously observed in biomass burning emissions. These compounds represent all the compound families as described in the main paper and are given in Table S4. Various mass loadings were injected onto separate blank

quartz fiber filters and analyzed with the TD-GC×GC EI-HRToFMS. The volume ratio between the total external standard peak and the nearest total internal standard peak were then correlated to the respective mass loading ratio. Example mass loading calibration curves are shown in Figure S3. In general, the linearity between mass loading and instrument response was good ($R^2 > 0.9$) over a wide range of normalized mass loadings; this may not be true at extremely low and high mass loadings for some compounds. Measured levoglucosan mass loadings did exceed the upper limits of the calibration curve for some of the conifer burns; in these cases, the calibration curve was extrapolated and may lead to higher uncertainty in levoglucosan EFs. Furthermore, several PAH external standard compounds showed poor linearity because their peaks in the chromatogram co-eluted with the nearest internal standard peak at high mass loadings. These high mass loading points were not taken into account for the calibration curve. This assumption is valid as the volumes of the PAH peaks were not observed during the FSL experiments to be within this high mass loading range.

Table S3 list of internal standards used on each sample

Internal Standard Compounds	
d3-vanillin	d4-4-methoxy-benzaldehyde
d6-syringic Acid	d8-anthraquinone
d8- methylcatechol	d4-phthalic acid
d3- vanillic Acid	d5-benzoic acid
d4-3-nitrobenzoic Acid	d5-C10 acid
d5- 4-hydroxybenzaldehyde	d12-C14 acid
d9-1-nitropyrene	d31-C16 acid
d26-C12 alkane	d35-C18 acid
d28-C13 alkane	d43-C22 acid
d30-C14 alkane	d7-cholesterol
d34-C16 alkane	d5-Cholestane
d38-C18 alkane	d5-3-hydroxy-1,5-pentanedioic acid
d42-C20 alkane	C6 diacid
d46-C22 alkane	d31-pentadecanol
d50-C24 alkane	$6^{13}C$ -glucose
d54-C26 alkane	$2^{13}C$-pentaerythritol
d58-C28 alkane	d10-pyrene
d62-C30 alkane	d10-phenanthrene
d66-C32 alkane	d12-perylene
d70-C34 alkane	d12-chrysene
d74-C36 alkane	d14-dibenzanthracene

Table S4 List of external standards used to determine the mass loading calibration curve of the TD-GC×GC-EI-HRToFMS

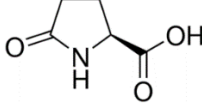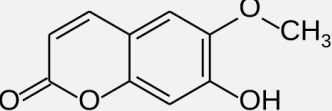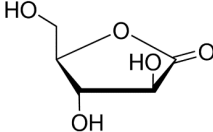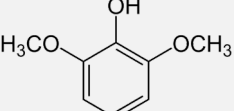| External Standard Compounds			
Cholesterol	Retene	C7 carboxylic acid	C12 alkane
Stigmasterol	Naphthalene	C8 carboxylic acid	C13 alkane
β-sitosterol	Phenanthrene	C9 carboxylic acid	C14 alkane
Ergosterol	Pyrene	C10 carboxylic acid	C15 alkane
α-Amyrin	Acenaphthene	C11 carboxylic acid	C16 alkane
Levoglucosan	Acenaphthylene	C12 carboxylic acid	C17 alkane
Levoglucosenone	Anthracene	C13 carboxylic acid	Pentadecane, 2,6,10,14-tetramethyl-
Mannosan	1,2-Benzanthracene	C14 carboxylic acid	C18 alkane
Galactosan	Benzo(a)pyrene	C15 carboxylic acid	Hexadecane, 2,6,10,14-tetramethyl-
Guaiacol	Benzo(b)fluoranthene	C16 carboxylic acid	C19 alkane
Syringol (2,6-Dimethoxyphenol)	Benzo(g,h,i)perylene	C17 carboxylic acid	C20 alkane
Syringic Acid	Benzo(k)fluoranthene	C18 carboxylic acid	C21 alkane
Syringaldehyde	Chrysene	C20 carboxylic acid	C22 alkane
Sinapinalehyde	Dibenz(a,h)anthracene	C22 carboxylic acid	C23 alkane
Vanillin	Fluoranthene	C23 carboxylic acid	C24 alkane
Vanillic acid	Fluorene	C24 carboxylic acid	C25 alkane
4-hydroxybenzoic acid	Indeno(1,2,3-cd)pyrene	C26 carboxylic acid	C26 alkane
p-Anisic acid (4-methoxybenzoic acid)	Maltol	C28 carboxylic acid	C27 alkane
3,5-dimethoxyphenol	5-(Hydroxymethyl) furfural	D-(+)-glucose	C28 alkane
Phthalic acid	4-Nitrocatechol	D-(+)-mannose	C29 alkane
Abietic acid	5-Nitrovanillin	L-(-)-mannose	C30 alkane
Isopimaric acid	2,4-Dinitrophenol	D-(+)-galactose	C31 alkane
Resorcinol		D-Pinitol	C32 alkane
Hydroquinone		Pyrocatechol	C33 alkane
4-Methylcatechol			C34 alkane
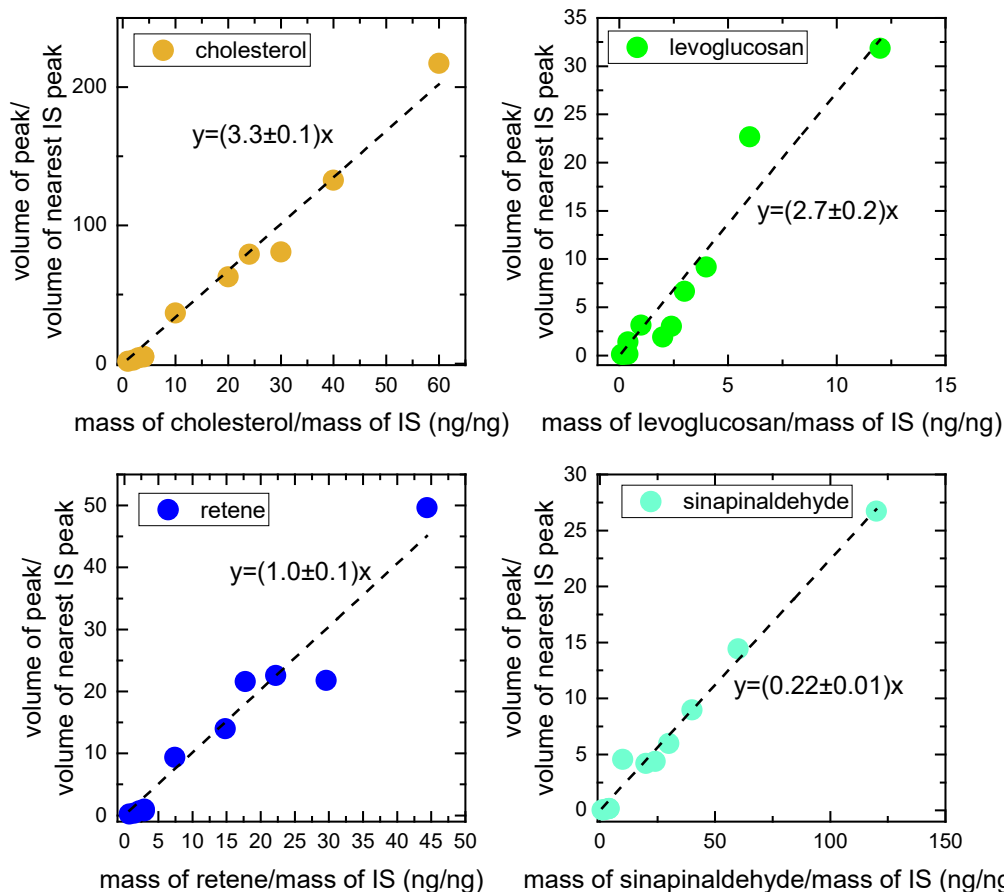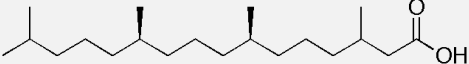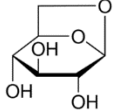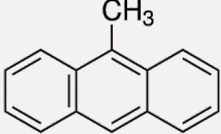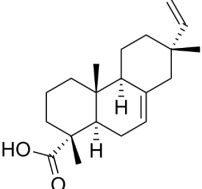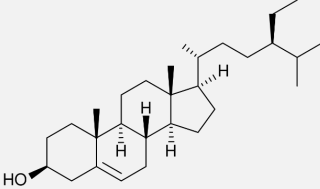
Figure S3 Example mass loading calibration curves for cholesterol, levoglucosan, retene, and sinapinaldehyde. Each external standard compound is normalized to the nearest internal standard (IS) compound. Colors are coded based upon the broad compound family: cholesterol=sterol, levoglucosan=sugar, retene=PAH, and sinapinaldehyde=methoxyphenol
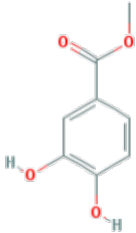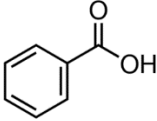
5. Classifying unidentified compounds into chemical families:

The 1D RI and the 2D retention time of an unidentified compound were first examined to ballpark potential family choices. Larger molecules like sterols have lower vapor pressures, and thus higher RI, than sugars. Derivatized methoxyphenols are more polar than derivatized sugars but have similar vapor pressures; therefore, methoxyphenols elute later in the second dimension than sugars. After the possible families were narrowed down, the electron ionization (EI) mass spectrum of the unidentified compound was then analyzed for specific ions and patterns that signify particular functional groups. For example, derivatized sugars exhibit 204 and 217 m/z and PAHs show little fragmentation. Derivatized sugars also show significant fragmentation with vacuum ultra violet light (VUV) ionization, making them easier to distinguish from compounds with benzene rings in the VUV mass spectrum. Each of the ~3000 compounds, including identified compounds, were analyzed using this method and placed into a family. Example compounds for each category are given in Table S5. The bulk of the unidentified compounds could not be placed into a category and remain unknown. More work needs to be done to synthesize standards of a wider variety of compounds in order to better identify/classify the unknown compounds.

Table S5 List of chemical families and examples for each family (without derivatization)

Family Name	Example compound (underivatized)
Non-cyclic aliphatic/oxygenated	3,7,11,15-tetramethyl hexadecanoic acid
Sugars	Levoglucosan
PAHs/methyl/oxygenated	1-Methylanthracene
Resin acids/diterpenoids	Isopimaric acid
Sterols/triterpenoids	β-Sitosterol
Organic nitrogen	Pyroglutamic acid
Aromatic oxygen heterocycles	Scopoletin
Oxygenated cyclic alkanes	Arabino-1,4-lactone
Methoxyphenols	Syringol

Substituted phenols	Methyl 3-4-dihydroxybenzoate	
Substituted benzoic acids	Benzoic Acid	

6. Classified I/SVOC mass fractions averaged over fuel type

The average mass fractions of total observed I/SVOCs for the chemical families across each fuel types (see Figure 3) are given in Table S5.

Table S6 Mass fraction (in %) and standard deviation of each of the chemical families for the various fuel types.

	Shrubs	**Grass**	**Wood**	**Coniferous Litter**	**Conifers**	**Peat**	**Dung**	**Coniferous Duff**	**Woody Debris**
Unknown	50%, 5%	60%, 6%	50%, 14%	50%, 9%	60%, 13%	50%	50%	60%, 15%	88%, 1%
Non-cyclic aliphatics/oxy	10%, 9%	8%, 2%	8%, 2%	7%, 2%	6%, 2%	26%	9%	9%, 2%	1%, 0%
Sugars	10%, 3%	12%, 2%	20%, 8%	15%, 6%	20%, 10%	3%	14%	10%, 6%	5%, 1%
PAH/methyl+oxy	1%, 1%	0%, 0%	1%, 1%	2%, 0%	1%, 0%	1%	0%,	2%, 0%	1%, 0%
Resin acids /diterpenoids	0%, 0%	0%, 0%	0%, 0%	8%, 1%	3%, 2%	0%	0%	3%, 2%	0%, 0%
Sterols, triterpenoids	1%, 0%	0%, 0%	0%, 0%	1%, 0%	0%, 0%	0%	1%	0%, 0%	0%, 0%
Organic nitrogen	13%, 8%	12%, 1%	8%, 4%	14%, 1%	10%, 5%	15%	22%	11%, 6%	1%, 1%
Oxy aromatic heterocycles	1%, 2%	1%, 0%	1%, 0%	0%, 0%	1%, 0%	0%	0%	0%, 1%	0%, 0%
Oxy cyclics	0%, 0%	3%, 2%	0%, 0%	1%, 0%	1%, 1%	0%	1%	1%, 1%	0%, 0%
Methoxyphenols	3%, 1%	3%, 2%	7%, 3%	3%, 0%	2%, 1%	4%	3%	4%, 1%	3%, 1%
Substituted phenols	7%, 0%	1%, 0%	0%, 0%	1%, 0%	1%, 1%	1%	1%	1%, 0%	0%, 0%
Substituted benzoic acids	1%, 1%	0%, 0%	0%, 0%	0%, 0%	0%, 0%	0%	0%	0%, 0%	0%, 0%
Average MCE.	0.958	0.898	0.958	0.955	0.931	0.840	0.902	0.871	0.878

7. EFs for families of compounds as a function of MCE:

Emission factors for each of the 12 families (including unknowns) were summed together in each fire-integrated sample. Figure S4 displays all of the family EFs as a function of modified combustion efficiency (MCE). This figure is an expansion of Figure 4 in the main paper. EFs for all chemical families exhibit a clear dependence on MCE, with smoldering burns producing 2-4 orders of magnitude more I/SVOC emissions. Logarithmic fits of the form log(EF)=slope(MCE)+int were also applied to these observations with the fit parameters displayed on each of the panels.
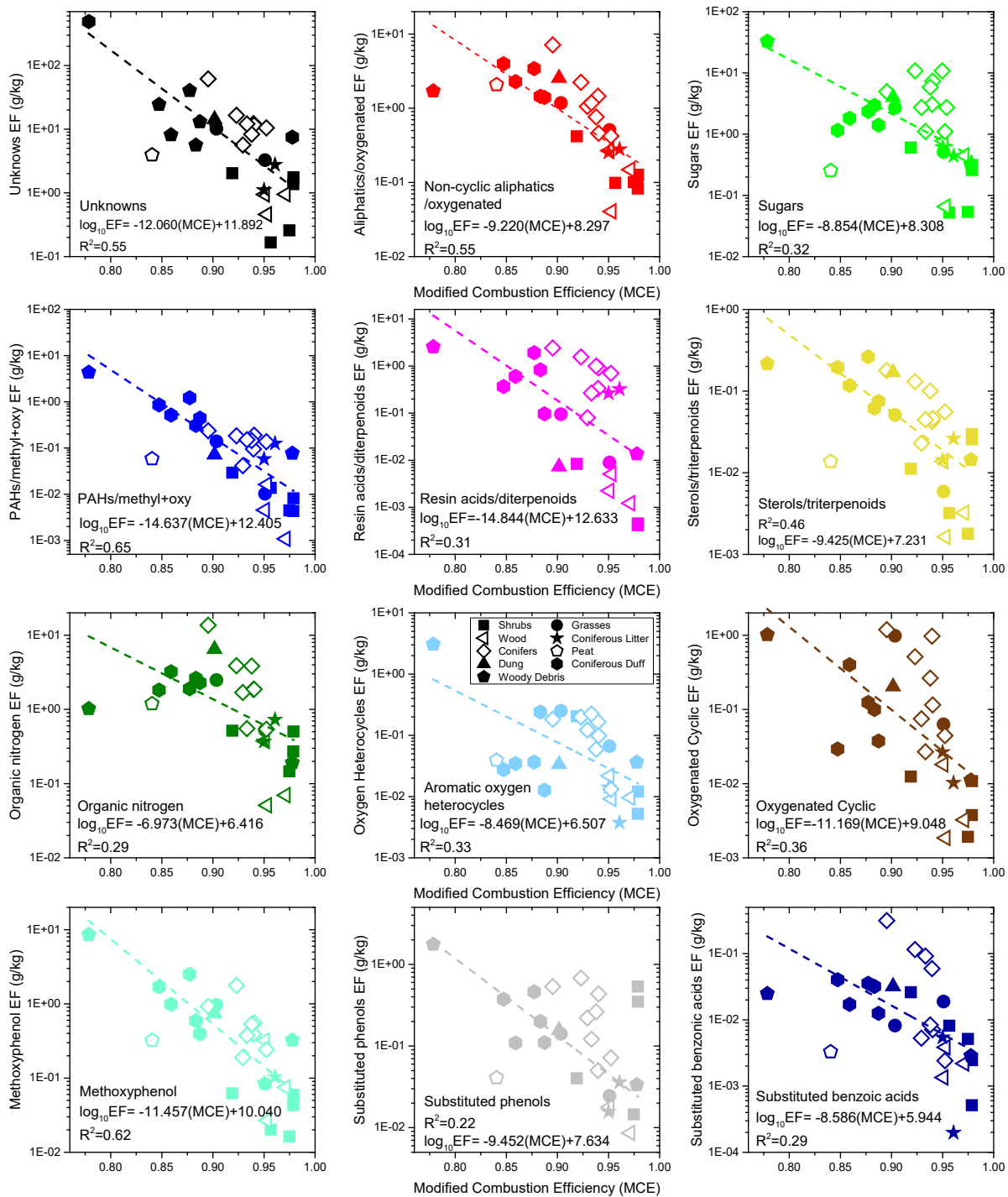
Figure S4 Emission factors (EFs) of each of the 12 chemical families as a function of modified combustion efficiency (MCE). Each panel/color represents a different chemical family and the different symbols show the different fuel types. Dashed lines are of the log(EF)=slope(MCE)+int fits with the parameters provided in the panel. Note, peat (open pentagon) was not included in the fits except for non-cyclics aliphatic/oxy (red).

Table S7 Logarithmic fit parameters for each of the chemical families and total I/SVOCs

Chemical Family	Slope ± error	Intercept ± error
Total	-11.44858 ± 1.87	11.58506 ± 1.74
Unknown	- 12.05974 ± 2.05	11.8919± 1.90
Non-cyclic Aliphatic/Oxy	-9.21952 ± 1.54	8.29706 ± 1.42
Sugars	-8.85359 ± 2.29	8.30773 ± 2.12
PAH/methyl+oxy	-14.63717± 2.07	12.40498± 1.91
Resin Acids/diterpenoids	-14.84408 ± 4.22	12.63297 ± 3.90
Sterols/triterpenoids	-9.42488 ± 1.93	7.23105 ± 1.79
Organic Nitrogen	-6.97334 ± 2.07	6.41579 ± 1.91
Oxy Aromatic Heterocycles	-8.46896 ± 2.33	6.50727 ± 2.15
Oxygenated Cyclic	-11.1686 ± 2.84	9.04829 ± 2.63
Methoxyphenol	-11.45675 ± 1.72	10.03962 ± 1.59
Substituted Phenol	-9.45183 ± 3.22	7.63392 ± 2.98
Substituted Benzoic Acid	-8.58551 ± 2.49	5.9437 ± 2.30

Works Cited:

Selimovic, V., Yokelson, R. J., Warneke, C., Roberts, J. M., de Gouw, J., Reardon, J. and Griffith, D. W. T.: Aerosol optical properties and trace gas emissions by PAX and OP-FTIR for laboratory-simulated western US wildfires during FIREX, Atmos Chem Phys, 18(4), 2929–2948, doi:10.5194/acp-18-2929-2018, 2018.

Ward, D. E. and Radke, L. F.: Emissions measurements from vegetation fires: A comparative evaluation of methods and results, Crutzen P J Goldammer J G Eds Fire Environ. Ecol. Atmospheric Clim. Importance Veg. Fires Dahl. Workshop Rep. Environ. Sci. Res. Rep. 13 Chischester Engl. John Wiley Sons P 53-76, 53–76, 1993.

Williams, B. J., Goldstein, A. H., Kreisberg, N. M. and Hering, S. V.: An in-situ instrument for speciated organic composition of atmospheric aerosols: Thermal Desorption Aerosol GC/MS-FID (TAG), Aerosol Sci. Technol., 40, 627–638, doi:10.1080/02786820600754631, 2006.

Yokelson, R. J., Griffith, D. W. T. and Ward, D. E.: Open-path Fourier transform infrared studies of large-scale laboratory biomass fires, J. Geophys. Res. Atmospheres, 101(D15), 21067–21080, doi:10.1029/96JD01800, 1996.